



MARMARA UNIVERSITY



FACULTY OF ENGINEERING

**OPTIMIZATION OF
SUSPENSION SYSTEM PARAMETERS FOR
ENHANCED RIDE COMFORT AND
STABILITY USING DOE**

Çiğdem GÜLER
Reyhan Ebrar TÜYSÜZ

GRADUATION PROJECT REPORT

Department of Mechanical Engineering

Supervisor

Dr. Berna BALTA

ISTANBUL 2025



MARMARA UNIVERSITY



FACULTY OF ENGINEERING

**OPTIMIZATION OF
SUSPENSION SYSTEM PARAMETERS FOR
ENHANCED RIDE COMFORT AND
STABILITY USING DOE**

Çiğdem GÜLER(150420997)
Reyhan Ebrar TÜYSÜZ(150419015)

GRADUATION PROJECT REPORT

Department of Mechanical Engineering

Supervisor

Dr. Berna BALTA

ISTANBUL 2025

ACKNOWLEDGEMENT

We would like to express our sincere gratitude to our advisor, Dr. Berna BALTA, for her guidance and support throughout the execution and completion of our senior design project titled “Optimization of Suspension System Parameters for Enhanced Ride Comfort and Stability using Design of Experiments (DOE)”.

Her academic mentorship, constructive feedback, and continuous support have greatly contributed to building the scientific foundation of our work and ensuring its proper progress.

We especially appreciate the valuable time she dedicated to reviewing our study and offering insightful suggestions, which have been instrumental in the development of our project.

June, 2025

Çigdem GÜLER

Reyhan Ebrar TÜYSÜZ

Table of Contents

ACKNOWLEDGEMENT.....	i
ABSTRACT.....	iv
SYMBOLS.....	v
ABBREVIATIONS	vi
TABLE OF FIGURES	vii
LIST OF TABLES.....	xi
1. INTRODUCTION	1
1.1 Fundamentals of Vehicle Suspension System	2
1.1.1 Springs	2
1.1.2 Dampers	4
1.1.3 Tires	5
1.1.4 Auxiliary Components of the Suspension System.....	5
1.2 Types of Suspension Systems.....	6
1.2.1 Active Suspension System.....	8
1.2.2 Semi-Active Suspension Systems.....	9
1.2.3 Passive Suspension Systems	9
1.3 Significance of Suspension System	10
2. MATERIAL AND METHOD	11
2.1 Quarter Car Suspension Model.....	11
2.2 Equation of Motion.....	13
2.3 Simulink.....	17
2.3.1 Excitation Signal and Parameter Definition	18
2.3.2 Output Signals, RMS Calculations, and Tire-Road Contact Force	20
2.3.3 Differential Equation-Based Modelling of the Quarter Car System.....	23

2.3.4	State-Space-Based Mathematical Modeling of the Quarter Car System	24
2.3.5	Transfer Function-Based Modeling of the Quarter Car System	27
3.	OPTIMIZATION USING DOE	30
3.1	The Definition and Aim of Optimization.....	30
3.1.1	Performance Metrics Considered in DOE	31
3.1.2	Optimization Approach Used	32
3.2	Design of Experiments (DOE) Application	33
3.2.1	Design of Experiment: Factors, Levels, and Method Selection.....	33
3.2.2	Analysis.....	34
3.2.3	Effect of DOE Results on Optimization	41
4.	RESULTS AND DISCUSSION.....	42
4.1	Model Verification Results.....	42
4.2	Parameter Effect Analysis.....	46
4.2.1	Effects of Spring Stiffness	46
4.2.2	Effects of Damping Coefficient	48
4.2.3	Effects of Tire Stiffness	51
4.3	Design of Experiment and Optimization Results.....	54
4.3.1	ANOVAMain Effect Plots.....	55
4.3.2	Response Optimizer Results	56
5.	CONCLUSION.....	59
6.	REFERENCES	60
7.	APPENDICES	64

ABSTRACT

Suspension systems are critical mechanical components in automotive engineering, directly affecting both ride quality and dynamic stability. This project presents the development and analysis of a passive quarter car suspension model to evaluate the vertical dynamics of a vehicle subjected to road disturbances. The model is constructed in MATLAB Simulink and incorporates key mechanical parameters such as spring stiffness, damping coefficient, sprung mass, and unsprung mass. A Design of Experiments (DOE) approach is implemented to perform a structured parametric analysis, enabling the identification of optimal parameter combinations that enhance system performance. The study aims to establish a balance between ride comfort and handling by systematically investigating the effects of design variables on the system's time-domain response. The results provide valuable insight into suspension behavior and form a foundation for future optimization and control strategies in vehicle dynamics.

SYMBOLS

m_a	: Vehicle body mass (sprung mass)
m_t	: Unsprung mass
k_t	: Tire stiffness
k_a	: Suspension stiffness
b	: Damping Coefficient
$y(t)$: Sprung mass vertical displacement
$\dot{y}(t)$: Sprung mass vertical velocity
$\ddot{y}(t)$: Sprung mass vertical acceleration
$x(t)$: Unsprung mass vertical displacement
$\dot{x}(t)$: Unsprung mass vertical velocity
$\ddot{x}(t)$: Unsprung mass vertical acceleration
$u(t)$: Road input (road profile)
F_t	: Tire-road contact force
RMS	: Root Mean Square value

ABBREVIATIONS

MATLAB : Matrix Laboratory

DOE : Design of Experiments

RMS : Root Mean Square

ANOVA: Analysis of Variance

ISO: Internal Organization for Standardization

FBD : Free Body Diagram

TF : Transfer Function

SS : State-Space

LTI : Linear Time-Invariant

Simulink : Simulation and Link Environment

TABLE OF FIGURES

Figure 1.1:The structure of a typical suspension [3].....	2
Figure 1.2:Coil Spring [4].....	3
Figure 1.3:Leaf Spring [4]	3
Figure 1.4:Torsion Bar [4]	4
Figure 1.5: Shock Absorber [5]	5
Figure 1.6: Vehicle Fixed Axes [6].....	6
Figure 1.7: Independent and Dependent Suspension Systems [8].....	7
Figure 1.8:Types of vehicle suspensions: (a) passive suspensions; (b) semi-active suspensions; (c) active suspensions [3].....	8
Figure 1.9:Active suspension system structures: a. Spring-assisted active model b. Fully active model [10]	8
Figure 1.10:Semi-active suspension system [13].....	9
Figure 1.11:Passive suspension system [13].....	10
Figure 2.1: Vehicle Suspension System Schematic.....	12
Figure 2.2:Quarter Car Model.....	14
Figure 2.3: Free Body Diagram for the Sprung Mass of the Quarter Car Model When Unsprung Mass Stationary.....	15
Figure 2.4:Quarter Car Model: Free Body Diagram When Sprung Mass Fixed	15
Figure 2.5: Unsprung Mass of the Quarter Car Model	16
Figure 2.6: Free Body Diagram for the Unsprung Mass of the Quarter Car Model (Sprung Mass Stationary)	16
Figure 2.7: Free Body Diagram for the Unsprung Mass of the Quarter Car Model (Unsprung mass fixed)	17
Figure 2.8: Differential Equation Based Simulink Model	24
Figure 2.9:Simulink Model Transfer Function Model.....	29
Figure 3.1:Experiment Matrix and Simulation Output	34
Figure 3.2:Pareto Graph for RMS of body acceleration	35
Figure 3.3: Pareto Chart after first iteration for RMS of Body Acceleration	35
Figure 3.4:Pareto Chart after second iteration for RMS of Body Acceleration.....	36
Figure 3.5:Pareto Graph Tire-Road Contact Force (peak to peak value)	37

Figure 3.6. Pareto Chart of after first iteration for Tire-Road Contact Force (peak to peak value).....	38
Figure 3.7:Pareto Chart of after second iteration for Tire-Road Contact Force (peak to peak).....	38
Figure 3.8 Analysis of Variance Results for Tire Road Contact Force (Peak to Peak)....	39
Figure 3.9 Pareto Graph Tire-Road Contact Force (RMS).....	39
Figure 3.10 After ABC eliminated for Tire-Road Contact Force (RMS).....	40
Figure 3.11 After AC eliminated for Tire-Road Contact Force (RMS)	40
Figure 3.12 Analysis of Variance Results for Tire Road Contact Force (RMS)	41
Figure 4.1: Sprung Displacements Graph.....	43
Figure 4.2:Sprung Displacements Graphs	44
Figure 4.3: Unsprung Displacements Graphic	45
Figure 4.4: Unsprung Displacements Graphics	45
Figure 4.5:Sprung Acceleration Graphic for Spring Stiffness =22000N/m	47
Figure 4.6: Sprung Acceleration Graphic for Spring Stiffness=16000N/m	47
Figure 4.7:Sprung mass acceleration for Damping Coefficient of 1000 Ns/m.....	48
Figure 4.8:Sprung Mass Acceleration for Damping Coefficient of 3000 Ns/m	49
Figure 4.9:Tire-Road Contact Force for Damping stiffness is equal to 3000 Ns/m.....	50
Figure 4.10:Tire-Road Contact Force for Damping Coefficient of 1000 Ns/m	50
Figure 4.11: Sprung Mass Aceleration for Tire Stiffness of 150000 N/m.....	51
Figure 4.12: Sprung Mass Aceleration for Tire Stiffness of 220000 N/m.....	52
Figure 4.13:Tire-Road Contact Force for Tire Stiffness of 150000 N/m	53
Figure 4.14:Tire-Road Contact Force for Tire Stiffness of 220000 N/m	53
Figure 4.15: Main Effect Plot for Body Acceleration.....	55
Figure 4.16: Main Effect Plot for Tire Contact Force Peak	55
Figure 4.17: Main Effect Plot for Tire Contact RMS	56
Figure 4.18 Response Optimizer Results.....	57
Figure 7.1 Graph for sprung mass acceleration with minimum variables	64
Figure 7.2 Cursor Measurements in Figure 7.1	64
Figure 7.3 Signal Statistics in Figure 7.1	64
Figure 7.4 Graph for sprung mass velocity with minimum variables.....	65

Figure 7.5 Cursor Measurements in Figure 7.4	65
Figure 7.6 Signal Statistics in Figure 7.4.....	65
Figure 7.7 Graph for sprung mass displacement with minimum variables	66
Figure 7.8 Cursor Measurements in Figure 7.7	66
Figure 7.9 Signal Statistics in Figure 7.7.....	66
Figure 7.10 Graph for unsprung mass acceleration with minimum variables	67
Figure 7.11 Cursor Measurements in Figure 7.10	67
Figure 7.12 Signal Statistics in Figure 7.10.....	67
Figure 7.13 Graph for unsprung mass velocity with minimum variables.....	68
Figure 7.14 Cursor Measurements in Figure 7.13	68
Figure 7.15 Signal Statistics in Figure 7.13	68
Figure 7.16 Graph for unsprung mass displacement with minimum variables	69
Figure 7.17 Cursor Measurements in Figure 7.16	69
Figure 7.18 Signal Statistics in Figure 7.16.....	69
Figure 7.19 Graph for sprung mass acceleration with maximum variables	70
Figure 7.20 Cursor Measurements in Figure 7.19	70
Figure 7.21 Signal Statistics in Figure 7.19	70
Figure 7.22 Graph for sprung mass velocity with maximum variables.....	71
Figure 7.23 Cursor Measurements in Figure 7.22	71
Figure 7.24 Signal Statistics in Figure 7.22	71
Figure 7.25 Graph for sprung mass displacement with maximum variables.....	72
Figure 7.26 Cursor Measurements in Figure 7.25	72
Figure 7.27 Signal Statistics in Figure 7.25	72
Figure 7.28 Graph for unsprung mass acceleration with maximum variables	73
Figure 7.29 Cursor Measurements in Figure 7.28	73
Figure 7.30 Signal Statistics in Figure 7.28.....	73
Figure 7.31 Graph for unsprung mass velocity with maximum variables	74
Figure 7.32 Cursor Measurements in Figure 7.31	74
Figure 7.33 Signal Statistics in Figure 7.31	74
Figure 7.34 Graph for unsprung mass displacement with maximum variables.....	75
Figure 7.35 Cursor Measurements in Figure 7.34	75

Figure 7.36 Signal Statistics in Figure 7.34	75
Figure 7.37 Graph for Tire Road Contact Force with maximum values	76
Figure 7.38 Cursor Measurements in Figure 7.37	76
Figure 7.39 Signal Statistics in Figure 7.37	76
Figure 7.40 Graph for Tire Road Contact Force with minimum values	77
Figure 7.41 Cursor Measurements in Figure 7.40	77
Figure 7.42 Signal Statistics in Figure 7.40	77

LIST OF TABLES

Table 1. Parameters for Boundaries [19] [17] [20].....	19
Table 2: RMS and Tire Road Contact Force Results.....	54

1. INTRODUCTION

With rapid advancements in technology, the automotive industry has made significant progress in vehicle dynamics and suspension systems. Modern suspension technologies, including air suspension and electronically controlled adaptive systems, have significantly improved both ride comfort and handling performance.

The suspension system plays a vital role in maintaining vehicle stability, absorbing shocks from road irregularities, and improving the overall driving experience.

Suspension system connects the wheel and the vehicle body by springs, dampers and some linkages, the spring carries the body mass by storing energy and helps to isolate the body from road disturbances, while damper dissipates this energy and helps to damp the oscillations. [1] [2]

Among the different types of suspension systems, passive suspension remains the most widely used due to its mechanical simplicity, cost-effectiveness and reliability. It consists of fixed elements such as springs and dampers that are not actively controlled but are designed to offer a compromise between comfort and handling. Although active and semi-active systems are becoming more common, passive suspension continues to serve as a benchmark in suspension studies and real-world applications.

Suspension performance is influenced by several key parameters, including spring stiffness, damping coefficient, and the distribution of sprung and unsprung masses. To study and optimize these parameters, simplified mathematical models such as the quarter car or half car model are often used. These models provide an effective framework for analyzing vehicle dynamics with reduced computational complexity.

In this project, a quarter car passive suspension model is developed using MATLAB/Simulink to simulate the vertical dynamics of a vehicle under road disturbances. The goal is to examine how variations in suspension parameters affect ride quality and road holding. A Design of Experiments (DOE) approach is used to systematically vary the spring stiffness, tire stiffness and damping coefficient, enabling efficient analysis of their individual and combined effects. This methodology helps identify optimal parameter combinations while reducing the number of required simulations.

1.1 Fundamentals of Vehicle Suspension System

The vehicle suspension system aims to absorb road irregularities, bumps, and pothole impacts, and to ensure tire grip on the road surface. The primary elements responsible for these functions are the springs, dampers and tires, which collaboratively manage wheel movement and maintain consistent road contact. Springs absorb and release energy to smooth out abrupt vertical forces acting on the vehicle, while dampers (shock absorbers) control this motion by dissipating energy and minimizing vibrations. Tires, serving as the interface between the vehicle and the road, are essential for both comfort and traction. These main components are supported by various structural parts such as control arms, stabilizer bars, and linkages, which help regulate wheel motion and enhance vehicle stability and handling.

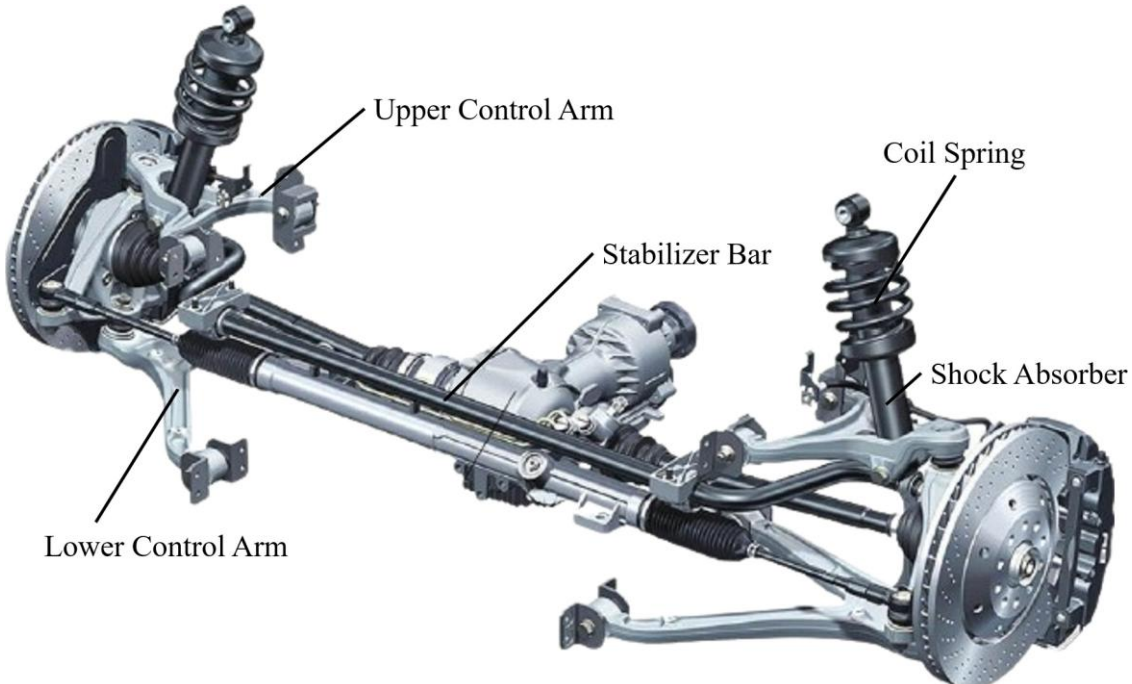


Figure 1.1:The structure of a typical suspension [3]

1.1.1 Springs

Springs act as reservoirs of energy. They store the energy due to the sudden force which comes when the vehicle encounters a bump or a pothole. This energy is released subsequently and with the action of dampers, the energy is converted into heat and bounce is avoided.

The action of springs can be understood by considering what happens when a vehicle encounters a bump or a pothole. When the vehicle hits a bump, the tire is suddenly pushed up. If there is rigid

suspension (without spring), the full force will be transferred to the carriage unit and push it up with almost no loss in force in the form of a shock or bounce. [4] Coil springs are the most commonly used spring type in today's passenger vehicles. Coil springs, which are wound in a helical shape, provide linear or progressive force depending on their geometry. They are made of hardened steel and are suitable for various ride and handling needs.



Figure 1.2:Coil Spring [4]

Leaf springs are mostly used for heavy vehicles such as trucks and commercial vehicles. They consist of flat metal plates stacked on top of each other. They can carry large loads. However, they are less comfortable compared to coil springs. Leaf springs also have different types within themselves.

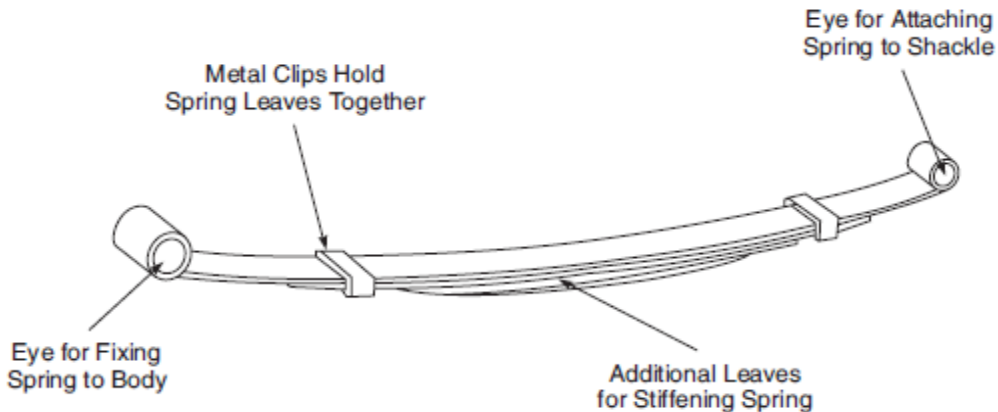


Figure 1.3:Leaf Spring [4]

Torsion bars act as suspension springs by twisting a metal bar. One end is connected to the vehicle chassis, and the other end is connected to the suspension with a lever. With the vertical movement

of the wheel, the twisting bar applies resistance. They are generally used in off-road and military vehicles.

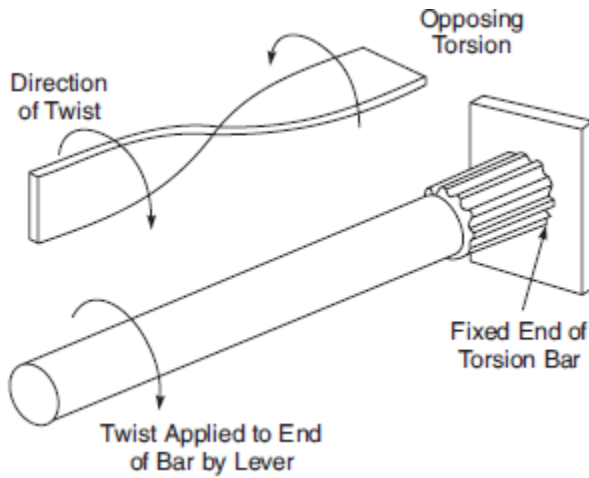


Figure 1.4:Torsion Bar [4]

Rubber springs are used more in commercial vehicles. Rubber is however used as bushes to check the transmission of vibration, for example, in the ends of a key spring. Rubber springs have been used only in a few cases in passenger cars since the precise control of ride essential for comfort is difficult to achieve with such springs.

In air and gas springs, compressed air or gas is filled in the cylinder or bellows against which the wheel movement is transmitted through a diaphragm. As soon as the wheel has passed over a road irregularity the compressed air pressure returns the system to its original position. [4]

1.1.2 Dampers

Dampers are used in the suspension system to check any continuous vibration which may follow the initial force on the spring. Damping action is provided by the absorption of kinetic energy, which is converted into heat through controlled fluid flow or internal component deformation. [4] Without dampers, the vehicle would continue its oscillatory motion due to the springs and would not stop. For this reason, the damper and spring need to function as a single unit. When designing the suspension system, the spring constant and the damping coefficient must be analyzed together. Determining these parameters is very important for both road holding and ride comfort. The main types of dampers are hydraulic shock absorbers, gas-filled shock absorbers, adjustable shock absorbers, and twin- or mono-tube shock absorbers. Hydraulic shock absorbers are the most

commonly used type for passive suspension systems. They generate resistance through the motion of a piston inside hydraulic fluid. As this fluid passes through narrow passages, it creates damping against oscillations and helps stabilize the vehicle. Therefore, damper design plays a critical role in shaping the overall dynamic behavior of the suspension system.

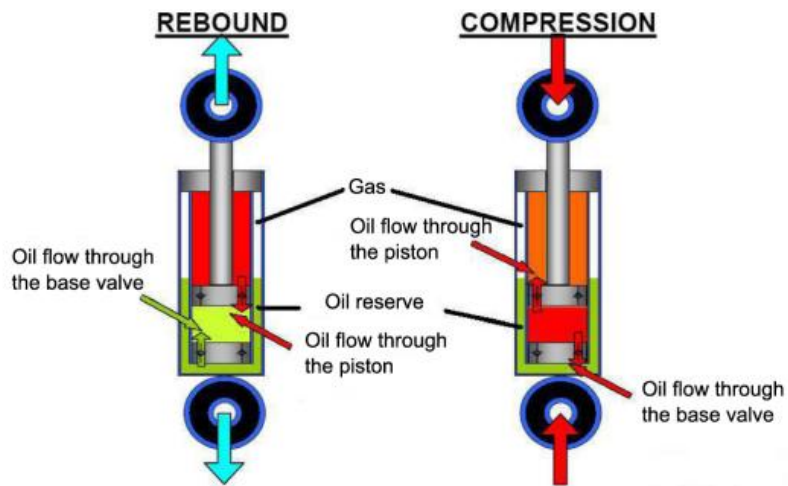


Figure 1.5: Shock Absorber [5]

1.1.3 Tires

Tires are the most important members in motor car transmission and drive system. Not only do they have to cope with the worst possible forces, shocks and other parameters, they are also expected to absorb most of them along with the suspension system so that the riders do not feel any of it. [4] The load they receive from the road is transferred to the suspension. Their elastic shapes and viscous properties act to damp the system. Tire stiffness and air pressure are required to provide road holding and driving comfort. Tires on a car are generally assumed to be linear springs with a constant spring rate. They are linearized for modeling and experiments in this way. However, in reality, they behave more complexly and nonlinearly.

1.1.4 Auxiliary Components of the Suspension System

Linkages, control arms, and anti-roll bars are important in the suspension system. Linkages and control arms connect the wheels to the vehicle chassis and determine wheel direction movement. These have a direct impact on directional stability of the vehicle through correct wheel alignment and suspension geometry. Adjustments in these mechanical parts provide parameters such as toe, camber, and caster. Proper suspension geometry delivers stable vehicle handling to steering and

maneuvering. Anti-roll bars are used to reduce body roll during cornering. They help by linking the left and right sides of suspension to share the load evenly should one wheel hit a bump. This improves vehicle stability and roadholding without significantly detracting from ride comfort. An anti-roll bar is a torsional spring that connects the left and right wheels through the suspension. Although independent suspensions allow each wheel to move separately, the anti-roll bar—hinged across the chassis and connected to the lower wishbones on each side—links the two sides by twisting under cornering forces to reduce body roll. [4]

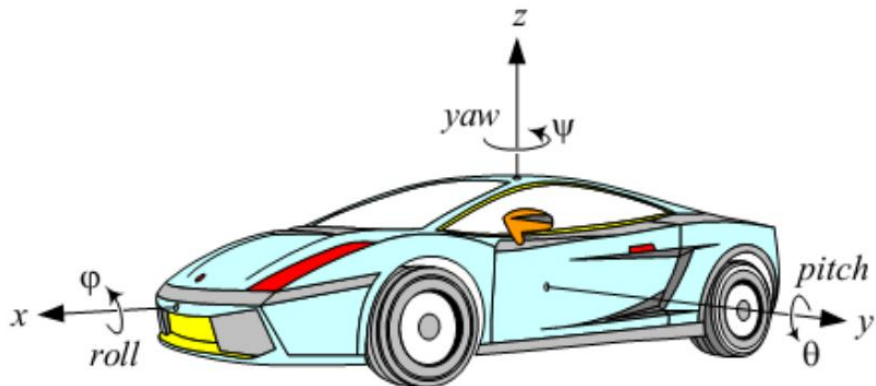


Figure 1.6: Vehicle Fixed Axes [6]

Here, in this study, vertical motions alone are considered since a quarter car model is used. The model simplifies the suspension to a two-degree-of-freedom system with only vertical dynamics in mind. Thus, no investigation has been carried out on caster, camber, and toe angles.

1.2 Types of Suspension Systems

Considering the mechanical structure, suspension systems can be grouped as dependent or independent. Independent suspension is a type of suspension system in which each wheel on the same axle can move vertically independently of the others. This configuration allows for better handling, improved ride comfort, and more consistent tire contact with the road surface. It is commonly used in the front axles of passenger cars and in performance vehicles due to its dynamic advantages. Dependent suspension generally has two main types include single or tandem axle

suspension systems. The most common types for typical single axle suspensions can be as leaf spring and trailing arm suspension. [4] [7]

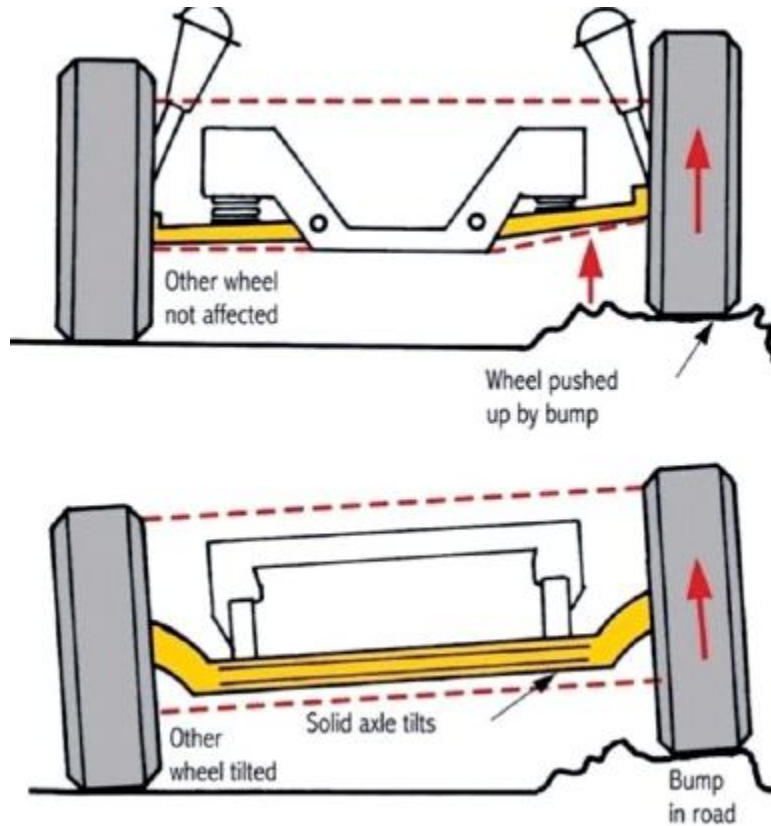


Figure 1.7: Independent and Dependent Suspension Systems [8]

Vehicle suspension systems are examined in three basic ways based on their vibration damping characteristics, whether originating from the road or driving style: **active, semi-active, and passive suspension systems.** [9]

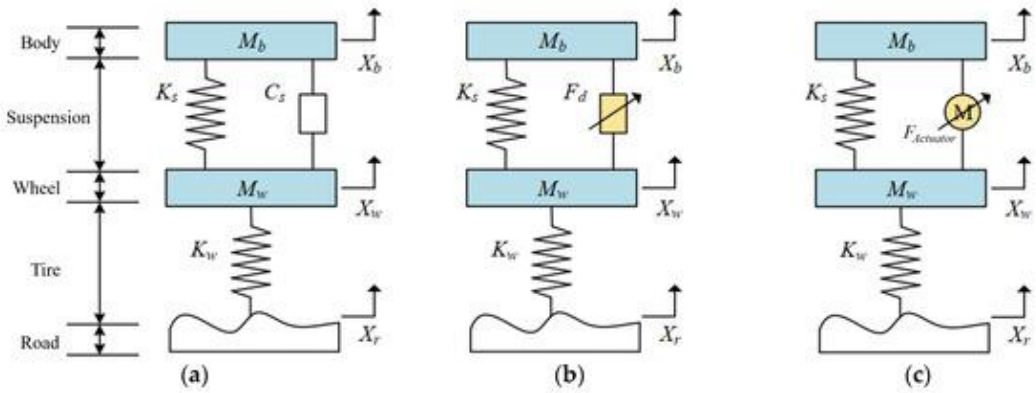


Figure 1.8:Types of vehicle suspensions: (a) passive suspensions; (b) semi-active suspensions; (c) active suspensions [3]

1.2.1 Active Suspension System

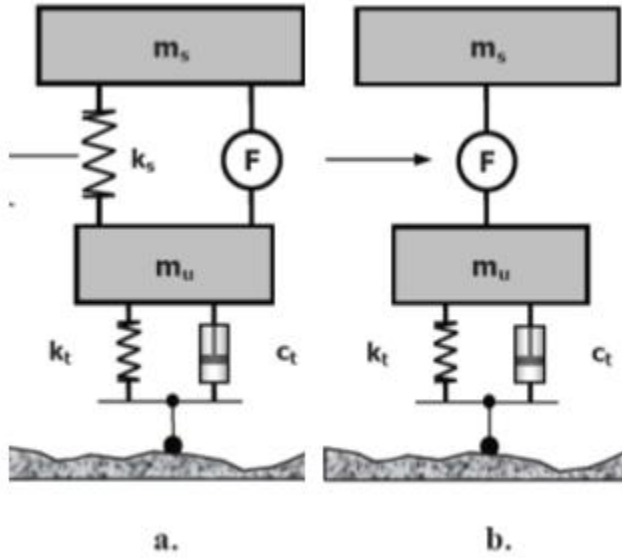


Figure 1.9:Active suspension system structures: a. Spring-assisted active model b. Fully active model [10]

Active suspension systems are sophisticated setups with the capacity to actively control the motion of suspension components. They typically use hydraulic or electromechanical actuators that directly alter the forces between the body and the wheel. Road conditions are read in real-time and the system continues to alter the suspension setup continuously by a control unit. Active suspensions yield optimum performance in comfort, handling, and roll control of the body. Despite the performance increase they offer, active suspension systems require an external energy source. This can lead to increased cost and a complex structure for vehicles using this type of suspension

system. [10] Active suspensions are used extensively in luxury vehicles, race cars, and systems with high dynamic accuracy.

1.2.2 Semi-Active Suspension Systems

Semi-active suspension systems have emerged as a promising alternative, striking a balance between the simplicity of passive systems and the adaptability of active systems. [11] [12]

Semi-active suspension systems are characterized by time-varying adjustable damping coefficient but fixed spring stiffness. Such systems employ electronically commanded dampers extensively, and they allow the suspension to switch between soft and hard modes with varying driving conditions.

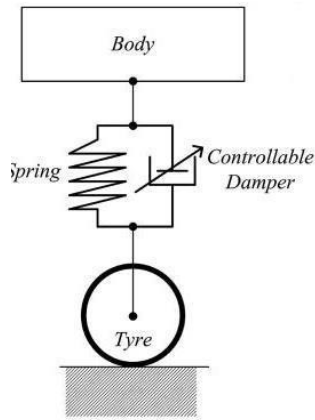


Figure 1.10:Semi-active suspension system [13]

One of the most widely applied technologies to semi-active systems is based on magnetorheological fluids—fluids that respond to a change in viscosity to a magnetic field and are able to switch instantly to damping response. These systems are finding a feasible balance between performance and price and are being used to an ever-growing extent in mid to high-end vehicles today.

1.2.3 Passive Suspension Systems

Passive suspension systems possess pre-determined, fixed spring and damping coefficients. Passive system designs are for a specific operating condition and do not have the ability to adjust their parameters according to the operating conditions. [14] They can not respond to externalities or road condition changes; their function depends solely on their mechanical configuration. As the

simplest form of suspension, they are still prevalent today due to their low cost, simplicity, and ease of maintenance. The springing may be a coil spring or torsion bar, and damping is provided by hydraulic shock absorbers. The system is adjusted to compromise ride comfort and handling stability; however, the compromise is not always satisfactory in every driving condition. Passive suspension systems do not have any feedback devices or electronic control.

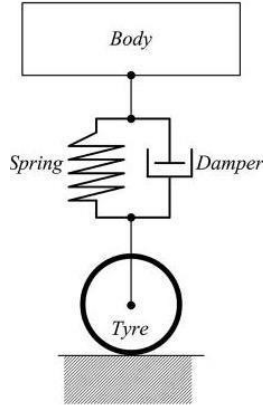


Figure 1.11:Passive suspension system [13]

Therefore, it becomes very critical to select appropriate spring stiffness and damping coefficients at the design level. Especially in quarter-car model studies, the vertical dynamic behaviour of the system is studied mathematically in an endeavour to achieve optimum comfort and stability. In this project as well, the analysis of the passive suspension system will be carried out with the aid of a quarter car model, and the effect of different spring and damping coefficients on the system response will be studied. In this regard, a number of design scenarios will be investigated for the improvement of suspension performance of modern vehicles.

1.3 Significance of Suspension System

Suspension systems are a critical system that has a direct impact on basic performance criteria such as ride comfort, road holding, directional stability, and safety within the scope of vehicle dynamics. The system dampens irregularities on the road surface and aims to reduce the vertical acceleration of the vehicle. It ensures constant contact of the wheels with the ground and aims to maintain the controllability of the vehicle. While the suspension fulfils these functions, it also regulates the distribution of dynamic loads on the vehicle. It supports both structural durability and driving performance.

The fundamental engineering problem during suspension design is to establish an optimum balance between road holding and driving comfort. A good suspension system must have springiness and damping. Springiness is elastic resistance to a load. On application of a sudden load the spring will compress/expand as the case may be without transmitting the same to the body. As the spring compression is complete it expands on rebound, and now damping becomes important since this will absorb the work energy as heat energy and the continuous oscillations of the spring which normally would have taken place are absorbed. [4]

An inadequate or incorrectly designed suspension system can cause skidding on curves, instability during braking, uneven tire wear, loss of grip, and failure of the vehicle to respond as expected in emergency situations. In addition, failure to effectively control oscillations on the vehicle can negatively affect the driver experience by increasing interior noise and vibration. This can increase driver fatigue, especially on long journeys, and therefore reduce safety.

The design of suspension systems should be evaluated by considering many parameters that affect the dynamic behavior of the vehicle. Variables such as vehicle mass, center of gravity, body rigidity and road conditions directly determine the performance of the suspension system. Therefore, suspension design should be considered not only as a mechanical structure but also as a whole in which engineering disciplines such as dynamic analysis, vibration control, material selection and optimization are evaluated together.

In conclusion, the suspension system is not just a comfort component. It is a subsystem that ensures the vehicle operates safely, stably, and efficiently throughout the journey. While a well-designed suspension system increases the vehicle's performance potential, a poorly designed system can seriously compromise user satisfaction and safety. For this reason, suspension design continues to be a high-priority area of research and development.

2. MATERIAL AND METHOD

2.1 Quarter Car Suspension Model

One of the most fundamental models used to analyze the vertical dynamic behavior of vehicle suspension systems is the quarter-car suspension model. This model represents only one wheel of the vehicle along with its associated suspension components.

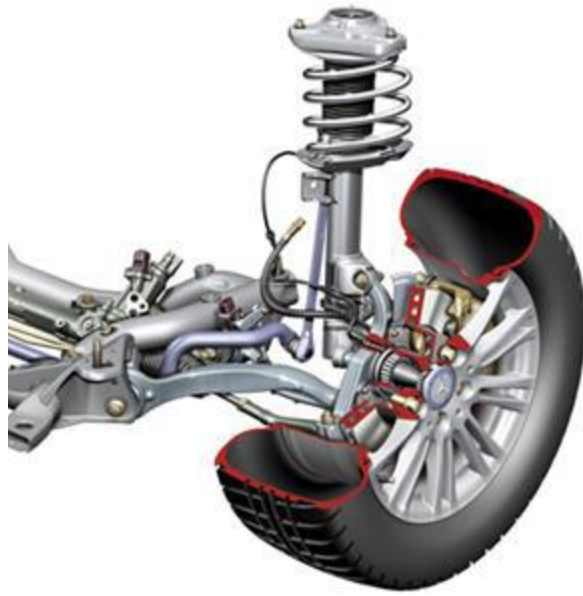


Figure 2.1: Vehicle Suspension System Schematic

It simplifies the full vehicle system to one-fourth of the actual structure, which significantly reduces complexity in mathematical modelling and numerical analysis while still capturing the essential dynamic behaviour. The quarter-car model is extensively used in both academic and industrial research due to its simplicity and capability to provide essential insights into ride comfort and road handling characteristics.

The model consists of two primary masses:

- The sprung mass (m_a), which represents the portion of the vehicle body supported by the suspension system.
- The unsprung mass (m_t), which includes the wheel, axle, and other components in direct contact with the road.

The system considers only vertical (z-directional) forces and motions. Horizontal and rotational dynamics are excluded to simplify the model and to focus on isolating and understanding vertical vibration behaviour caused by road irregularities. It is assumed that the road excitation is uniform across the tire contact patch and that the suspension system behaves in a linear manner under small displacement assumptions.

A spring is located between the sprung and unsprung masses, and its stiffness is characterized by the spring constant k_a . The spring generates an elastic force between the two masses, resisting oscillatory motion. A damper (shock absorber) is also placed between the same two masses and generates a damping force proportional to their relative velocity. The damping is quantified by the damping coefficient b .

Additionally, a tire is modeled as another spring element between the unsprung mass and the road surface, with its stiffness denoted as k_t . The road profile, including irregularities such as bumps or potholes, is modeled as an external input to the system, represented by $u(t)$.

The displacement variables used in the model are as follows:

- $y(t)$: vertical displacement of the sprung mass (m_a),
- $x(t)$: vertical displacement of the unsprung mass (m_t),
- $u(t)$: vertical displacement of the road surface (input).

The behavior of the system is governed by Newton's Second Law of Motion, which states that the net force acting on a body is equal to the product of its mass and acceleration: [15]

$$F = ma \quad (2.1)$$

By applying this fundamental principle to each mass in the system, second-order differential equations are derived. These equations describe the time-dependent dynamic response of the system and can be solved analytically or numerically.

2.2 Equation of Motion

In the current study, the motion equations required to create the quarter car model have been examined. The motion will only occur in the vertical plane. The free body diagram is analyzed as follows:

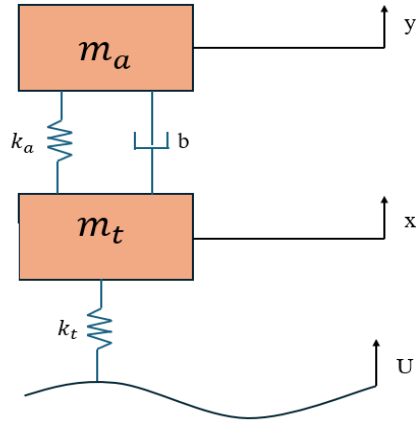


Figure 2.2:Quarter Car Model

As shown in the figure 2.2 , the motion equations for the quarter-car vehicle model are derived using the sprung mass (m_a), unsprung mass (m_t), damping coefficient (b), suspension spring constant (k_a), and wheel spring constant (k_t). The motion equations describe the vertical oscillations of the sprung mass.

The fundamental law from which most vehicle dynamics analysis begin is the second law formulated by Sir Isaac Newton: [15]

$$F = ma \quad (2.2)$$

When deriving the motion equations, the vehicle and wheel masses must be considered separately. In the case of the sprung and unsprung masses, two scenarios are analysed. The first case involves the unsprung mass being fixed while the vehicle moves upward. The second scenario involves the sprung mass being fixed while the unsprung mass moves upward.

Sprung Mass Analysis

If m_t is stationary and m_a is moving upwards:

In the first case, in response to the upward movement of the vehicle, seen in Figure 2.3, forces are applied in the downward direction by the spring and damper. The spring force is displacement-dependent, whereas the force exerted by the damper is directly proportional to the velocity. Additionally, the displacement acceleration of the vehicle mass generates a downward force.

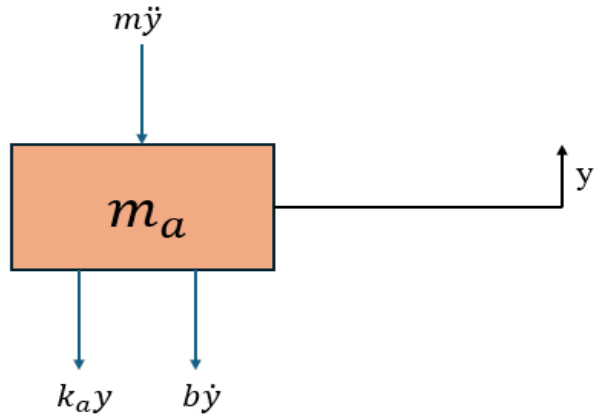


Figure 2.3: Free Body Diagram for the Sprung Mass of the Quarter Car Model When Unsprung Mass Stationary

If m_a is stationary and m_t is moving upwards:

In the case where the vehicle mass is fixed, due to the upward movement of the unsprung mass, seen in Figure 2.4. Both the spring and damper exert upward forces.

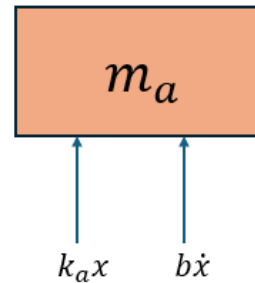


Figure 2.4:Quarter Car Model: Free Body Diagram When Sprung Mass Fixed

Based on the force diagrams developed, the equation of motion for the sprung mass is derived as follows:

$$m\ddot{x} + b\dot{x} + cx = 0 \quad (2.3)$$

$$m_a \ddot{y} + k_a(y - x) + b(\dot{y} - \dot{x}) = 0 \quad (2.4)$$

Unsprung Mass Analysis

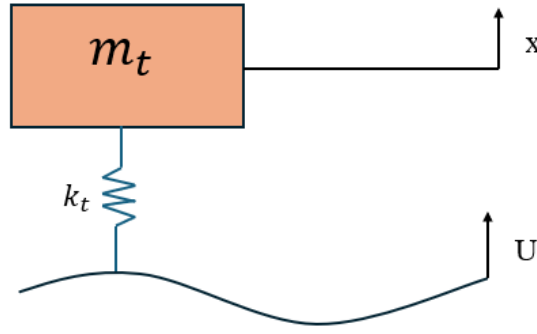


Figure 2.5: Unsprung Mass of the Quarter Car Model

When analysing the unsprung mass for the first case, it is assumed that the sprung mass is fixed while the unsprung mass moves upward in Figure 2.5. The forces acting on the mass in this scenario include the downward forces exerted by the suspension spring and damper, the weight of the wheel, the force generated by the displacement acceleration, and the force due to the wheel's own stiffness. In the upward direction, the reaction force from the road is considered.

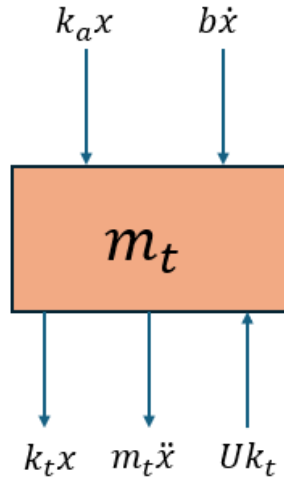


Figure 2.6: Free Body Diagram for the Unsprung Mass of the Quarter Car Model (Sprung Mass Stationary)

In the other case to be analysed, the unsprung mass is assumed to be fixed, and the upward movement of the sprung mass is considered. The forces applied in this scenario are the upward forces from the spring and damper, which are associated with the upward motion of the vehicle.

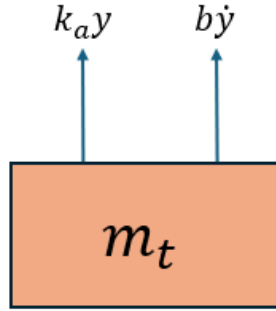


Figure 2.7: Free Body Diagram for the Unsprung Mass of the Quarter Car Model (Unsprung mass fixed)

Using the obtained forces, the equation of motion for the wheel mass is expressed as follows, and consequently, the displacement of the wheel can be calculated.

$$m_t \ddot{x} + k_t x + k_a x + b \dot{x} - U k_t - k_a y - b \dot{y} = 0 \quad (2.5)$$

$$m_t \ddot{x} + k_a(x - y) + b(\dot{x} - \dot{y}) = k_t(U - x) \quad (2.6)$$

2.3 Simulink

In this section, the time-dependent dynamic behavior of the quarter car suspension system is modeled and analysed using the MATLAB/Simulink environment. Simulink is a powerful engineering tool that enables visual, block diagram-based modeling of the time-varying responses of physical systems. It is widely used in modeling multi-domain systems that include both linear and nonlinear components, particularly in the modeling of vehicle suspension systems.

The model developed in this study consists of fundamental physical components such as the sprung mass, unsprung mass, suspension spring, damper, and tire stiffness. The force interactions between these components are established based on Newton's Second Law of Motion. The system dynamics defined by differential equations are modelled in Simulink using three different methods: transfer function, state space, and differential equation-based model approaches. The use of these three distinct modelling techniques on the same system provides a means of verification, ensuring that the results are consistent and reliable across different mathematical representations.

All three models are subjected to the same input signal—a sinusoidal road profile with a specified amplitude and frequency. By keeping the input conditions identical, the outputs obtained from

each model—including displacement, velocity, and acceleration values—are compared in a systematic manner. This comparison allows for the evaluation of the consistency between the different modelling approaches and enhances the overall reliability of the results. Demonstrating that different modelling techniques yield similar outputs for the same physical system serves as an important indicator of the model's accuracy and robustness.

To quantitatively assess ride comfort, the RMS value of the acceleration signal obtained from the sprung mass is calculated. The RMS represents the average vibration level over a specified period and is recognized as a reliable metric for comfort analysis. Additionally, the tire-road contact force is calculated based on the acceleration of the unsprung mass. This force characterizes the dynamic interaction between the tire and the road surface and is critical for evaluating road-holding performance. The calculated tire-road contact force is further analyzed by computing both its RMS and peak-to-peak values. While the RMS value provides insight into the overall stability of the tire-road interaction over time, the peak-to-peak value highlights the maximum fluctuation range of the force, reflecting extreme variations that can affect vehicle stability. These metrics are essential in assessing road handling performance, as they quantify the tire's ability to maintain consistent contact with the road surface under dynamic conditions.

The Simulink model offers a flexible and structurally consistent framework that supports parametric flexibility and allows for experimentation under various scenario conditions. This makes it particularly suitable for optimization studies and Design of Experiments (DOE) applications, providing a solid foundation for further system performance enhancements.

In the following subsections, the details of the differential equation-based, state-space-based, and transfer function models and input signal configuration. Additionally, RMS body acceleration, RMS tire road contact force and the tire-road contact force peak to peak calculations for these models will be presented individually.

2.3.1 Excitation Signal and Parameter Definition

The selection of appropriate parameters is crucial for a realistic analysis of the suspension system. First, the parameters to be treated as variables in this study were selected. While the weight of the vehicle and the wheel were kept constant, it was decided to vary the spring stiffness, tire stiffness, and damping coefficient. The effects of these three variables on the suspension system were then

analyzed. For each of these three variables, lower and upper bounds were determined. This approach aimed to ensure that the DOE analysis could be conducted smoothly. The values selected based on the literature review are presented in the table below. [16] [17] [18]

Table 1. Parameters for Boundaries [19] [17] [20]

Parameters	Lower Boundary	Upper Boundary
Tire Stiffness [N/m]	150000	220000
Spring Stiffness [N/m]	16000	22000
Damping Coefficient [Ns/m]	1000	3000

After determining the variable parameters and their corresponding ranges, the sprung and unsprung masses of the vehicle were selected based on a review of the literature. As a result, the values of **250 kg** for the sprung mass and **50 kg** for the unsprung mass were adopted. These values fall within the typical range for passenger cars, ensuring that the suspension model accurately represents realistic vehicle dynamics. [17] [21]

In order to analyze the dynamic response of the quarter-car suspension system, an external excitation must be applied to the system. In this study, a sinusoidal input signal representing typical road surface irregularities was chosen as the external excitation. This type of signal is commonly used because it allows for the evaluation of periodic responses, observation of resonance behavior, and assessment of ride comfort. Moreover, using a sinusoidal road input facilitates the analytical investigation of the system's frequency response and enables comparative analysis across different suspension configurations. This approach standardizes the model validation process as opposed to using more complex inputs such as ISO road profiles. The selection of the appropriate excitation frequency is crucial in evaluating the vibration characteristics of vehicle suspension systems. One of the most critical dynamic behaviors affecting ride comfort and road-holding performance is the system response near the natural frequency of the sprung mass. According to classical vehicle design principles, the sprung mass natural frequency suspension system must be within 1 Hz to 2 Hz. [22] [15]

The parameter values used in this study are as follows:

- Amplitude (A): 0.02 m
- Frequency (f): 1 Hz

This signal was directly applied to the unsprung mass, and the system's response to road-induced vibrations was observed. Particularly, the RMS values of the signals were used to assess the ride comfort performance and road handling under this input.

Defining the sinusoidal input parameters based on literature enhances the model's validity and enables direct comparison with similar studies.

2.3.2 Output Signals, RMS Calculations, and Tire-Road Contact Force

During the modelling process, various output signals were evaluated to analyze the dynamic response of the system. These outputs were primarily monitored through the acceleration of the sprung mass and the displacement of unsprung mass. The acceleration is particularly important as a quantitative indicator of ride comfort. Besides, the displacement is important for the road handling. In this context, the RMS values were calculated to determine the vibration level of the system.

Monitored Outputs:

- Displacement of the sprung mass, $y(t)$
- Acceleration of the sprung mass, $\ddot{y}(t)$
- Displacement of the unsprung mass, $x(t)$
- Acceleration of the unsprung mass, $\ddot{x}(t)$

These signals were directly obtained from the system blocks within the Simulink model.

Calculation of RMS:

In the analysis of ride quality and road handling, RMS calculations are widely used as an objective measure to quantify the vibration level transmitted to the vehicle body. This metric provides a single representative value of the overall vibration intensity over a specified time period or frequency range. [15]

RMS represents the average energy level of a time-varying signal. In terms of ride comfort analysis, it is used to assess the average vibration intensity experienced by passengers.

Mathematically, it is defined as follows:

$$RMS = \sqrt{\frac{1}{T} \int_0^T [f(t)]^2 dt} \quad (2.7)$$

This expression represents the square root of the mean of the squares of the selected signal over a given time interval. In this study, the vertical acceleration of the sprung mass, $\ddot{y}(t)$ and tire-road contact force F_t were used to calculate the RMS value.

Use of the RMS block:

The RMS values of the signals were calculated using the RMS blocks. The fundamental frequency was specified.

A high RMS value indicates that the system transmits more vibrations and experiences greater fluctuations in tire-road contact force, resulting in reduced ride comfort and weaker road handing. Conversely, a low RMS value suggests that the system provides better damping, isolates vibrations from the passenger, and maintains more stable tire contact with the road. Therefore, the RMS value was considered a key performance criterion throughout the experimental and optimization process, both for body acceleration and tire-road contact force.

Calculation of Tire-Road Contact Force:

Tire-road contact force is a critical performance indicator for vehicle road-holding and driving stability. This force directly reflects the interaction between the vehicle's wheels and the road surface, ensuring the vehicle's safe and balanced progression, especially under dynamic driving conditions (such as cornering, braking, and accelerating).

Mathematically, tire-road contact force (F_t) is generally defined as the vertical interaction force between the tire and the road, and in its most general form, it can be expressed in a suspension model as follows:

$$F_t = k_t(x(t) - u(t)) + c_t(\dot{x}(t) - \dot{u}(t)) \quad (2.8)$$

Where;

- k_t : Tire stiffness
- c_t : Tire damping coefficient
- $x(t)$: Vertical displacement of the unsprung mass (wheel)
- $u(t)$: Vertical displacement of the road profile (road input)
- $\dot{x}(t)$: Vertical velocity of the unsprung mass
- $\dot{u}(t)$: Vertical velocity of the road profile

However, in this study, since the tire damping coefficient (c_t) and thus the velocity-dependent damping term were not utilized in the modelling, the tire-road contact force equation was simplified as follows:

$$F_t = k_t(x(t) - u(t)) \quad (2.9)$$

The peak-to-peak value can be calculated as follows:

$$F_t(\text{peak to peak}) = F_{t,\max} - F_{t,\min} \quad (2.10)$$

The tire-road contact force was obtained in the Simulink model using blocks that simulate the interaction between the wheel and the road. This force is directly calculated based on the vertical stiffness of the tire.

High fluctuations in the tire-road contact force—reflected by a large peak-to-peak value—negatively affect vehicle stability and reduce road-holding performance. In contrast, a smaller peak-to-peak value indicates a more stable and consistent tire-road contact, which contributes to improved driving stability and better handling. Therefore, the peak-to-peak value of the tire-road contact force was considered a key performance criterion during both the experimental and optimization stages.

Additionally, the RMS value of the tire-road contact force is an important indicator that reflects the overall magnitude and consistency of the contact force over time. A higher RMS value indicates that the tire maintains a continuous and strong contact with the road surface, thereby enhancing traction effectiveness. This is particularly beneficial for improving vehicle control during dynamic maneuvers or over uneven terrain. Therefore, the RMS value was also used as a

complementary performance criterion, with the objective of maximizing it to evaluate and optimize the behavior of the suspension system.

2.3.3 Differential Equation-Based Modelling of the Quarter Car System

In this section, the quarter vehicle suspension system is modeled and analyzed in the MATLAB/Simulink environment using a differential equation-based approach. The model incorporates key components such as the sprung and unsprung masses, suspension spring, damper, and tire stiffness, which collectively represent the physical dynamics of the system.

The modelling process is based on the equations of motion derived in the previous section. These differential equations were implemented in Simulink using structured block diagrams. Specifically, integrator, gain, and summation blocks were utilized to represent the mathematical relationships between the system variables

The model consists of two primary masses:

- **Sprung mass:** Representing the vehicle body.
- **Unsprung mass:** Representing the wheel and associated components.

The interaction between these two masses is governed by the suspension spring and damper, while the interface between the unsprung mass and the road is modeled through tire stiffness. A sinusoidal displacement input simulates the road profile and is applied using a Sine Wave block.

In this model, the forces acting on each mass are used to generate acceleration, which is then integrated sequentially to obtain velocity and displacement using two integrator blocks. Each physical component has been modeled individually using Simulink blocks, enabling a detailed observation of the system's time-dependent dynamic behavior.

The sine wave input acts as the primary disturbance, influencing the tire stiffness and thereby generating force on the unsprung mass. The resulting motion responses—displacement, velocity, and acceleration—of both sprung and unsprung masses were observed using Scope blocks.

Key output of the system is the tire-road contact force, calculated by multiplying the unsprung mass's acceleration with its mass. This was implemented with a gain block in Simulink. The resulting force represents the dynamic interaction between the wheel and the road, serving as a

critical indicator of traction and stability. It also provides insight into the system's transient responses to road disturbances.

The acceleration of the sprung mass and tire-road contact force were further processed with a RMS block to evaluate ride comfort and road handling. The RMS value provides a quantitative measure of vibration intensity by computing the square root of the time-averaged squared signal. This value reflects the perceived comfort level and road handling during vehicle operation. The overall model structure is illustrated in the figure below.

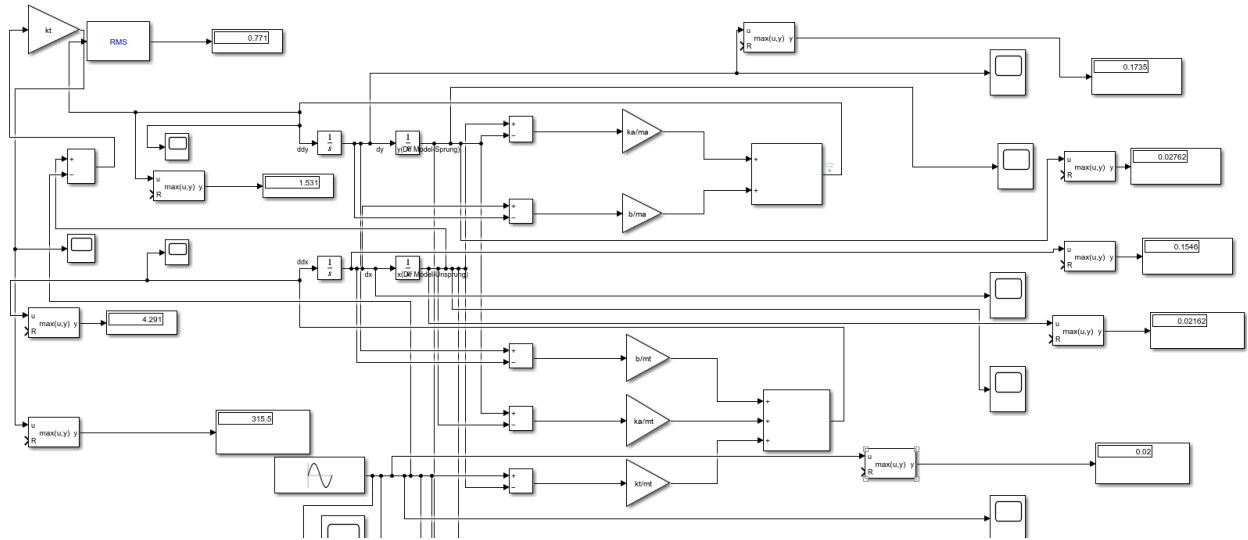


Figure 2.8: Differential Equation Based Simulink Model

2.3.4 State-Space-Based Mathematical Modeling of the Quarter Car System

This section explains how a quarter-car suspension system is represented using a mathematically based modelling approach, specifically through the state-space method, and how this model is implemented in the Simulink environment.

Mathematical modelling aims to describe the behavior of physical systems using mathematical structures such as differential equations, matrix representations, or transfer functions. Instead of modelling physical components with direct visual blocks, this approach employs an abstract mathematical representation of the system. As a result, the system dynamics can be addressed in a more concise and compact manner.

The state-space model has been applied to the quarter car vehicle model. This model helps in the easy analysis of the system and facilitates the analysis of the time-dependent results of the inputs. The first step here is the rearrangement of the equations using state variables. The state variables are provided below.

$$m_a \ddot{y} + b\dot{y} + k_a y - b\dot{x} - k_a x = 0 \quad (2.11)$$

$$m_t \ddot{x} + b\dot{x} + (k_a + k_t)x - b\dot{y} - k_a y = k_t U \quad (2.12)$$

The notations used are as follows:

$$\ddot{y} \rightarrow \dot{y}, y$$

$$\ddot{x} \rightarrow \dot{x}, x$$

The notations have been converted into the following condition:

$$\begin{array}{ll} x_1 = y & \dot{x}_1 = x_2 \\ x_2 = \dot{y} & \dot{x}_2 = \ddot{y} \\ x_3 = x & \dot{x}_3 = x_4 \\ x_4 = \dot{x} & \dot{x}_4 = \ddot{x} \end{array}$$

The equations related to the state variables for the equations 2.10 and 2.11 have been calculated as follows:

$$\dot{x}_2 = \frac{-b}{m_a}x_2 - \frac{k_a x_1}{m_a} + \frac{bx_4}{m_a} + \frac{k_a x_3}{m_a} \quad (2.13)$$

$$\dot{x}_4 = \frac{-b}{m_t}x_4 - \frac{(k_a + k_t)}{m_t}x_3 + \frac{b}{m_t}x_2 + \frac{k_a}{m_t}x_1 + \frac{k_t}{m_t}U \quad (2.14)$$

The general representation of the input and output matrices are as follows:

$$\text{Input Matrix: } \dot{x} = Ax + BU \quad (2.15)$$

$$\text{Output Matrix: } \dot{y} = Cx + DU \quad (2.16)$$

The formulations, arranged in matrix form, are presented as follows:

$$\begin{bmatrix} \dot{x}_1 \\ \dot{x}_2 \\ \dot{x}_3 \\ \dot{x}_4 \end{bmatrix} = \begin{bmatrix} 0 & 1 & 0 & 0 \\ -k_a & -b & k_a & b \\ \frac{-k_a}{m_a} & \frac{-b}{m_a} & \frac{k_a}{m_a} & \frac{b}{m_a} \\ 0 & 0 & 0 & 1 \\ \frac{k_a}{m_t} & \frac{b}{m_t} & \frac{-(k_a + k_t)}{m_t} & \frac{-b}{m_t} \end{bmatrix} \times \begin{bmatrix} x_1 \\ x_2 \\ x_3 \\ x_4 \end{bmatrix} + \begin{bmatrix} 0 \\ 0 \\ 0 \\ \frac{k_t}{m_t} \end{bmatrix} \times U$$

$$y = \begin{bmatrix} 1 & 0 & 0 & 0 \\ 0 & 0 & 1 & 0 \end{bmatrix} \times \begin{bmatrix} x_1 \\ x_2 \\ x_3 \\ x_4 \end{bmatrix} = \begin{bmatrix} x_1 \\ x_3 \end{bmatrix}$$

The integration of this model into the Simulink environment was achieved by entering the A, B, C, and D matrices into the State-Space block. A sine wave block with a specified amplitude and frequency was used as the input signal for the model. This signal was applied uniformly across all models for verification purposes, and the same sine wave block was directly connected to the input of the state-space-based model. In this way, all modeling approaches were exposed to the same road input.

The system outputs consist of the displacements of the sprung and unsprung components. These outputs were connected to the same Scope block as in the physical model, allowing for a graphical comparison to evaluate the model's accuracy.

Representing the state-space model using the State-Space block in Simulink enabled the system to be modeled while preserving both accuracy and simplicity. This block facilitated the representation of the entire system within a single structure, greatly simplifying model adjustments, parameter modifications, and testing of different state-space configurations.

In conclusion, although this modeling approach is more abstract compared to the physical model, it accurately represents the same system behavior. The consistency of the output responses between this model and the physical model strongly supports the validity of the state-space representation.

2.3.5 Transfer Function-Based Modeling of the Quarter Car System

The equations of motion for the quarter car vehicle model system were examined in the previous section. To perform the dynamic analysis of the system and model this quarter suspension system, the transfer function has been developed.

In addition to the differential equation, the transfer function is another way of mathematically modeling a system. The model is derived from the linear, time-invariant differential equation using what we call the Laplace transform. [23] For the purpose of simplifying the analysis of the system, the Laplace transform is applied. Time-dependent domains are converted into the frequency domain.

$$\frac{x(s)}{U(s)}, \frac{y(s)}{U(s)} \rightarrow \text{Transfer Functions}$$

$$x(t) = x(s) \quad (2.17)$$

$$\dot{x}(t) = sx(s) - x(0) \quad (2.18)$$

$$\ddot{x}(t) = s^2x(s) - sx(0) - x'(0) \quad (2.19)$$

It is assumed that:

$$x(0) = 0$$

$$x'(0) = 0$$

Then the frequency domains are as follows:

$$x(t) = x(s)$$

$$\dot{x}(t) = sx(s)$$

$$\ddot{x}(t) = s^2x(s)$$

$$y(t) = y(s)$$

$$\dot{y}(t) = sy(s)$$

$$\ddot{y}(t) = s^2y(s)$$

Using the equation 2.4, the formula obtained after applying the Laplace transform is as follows:

$$m_a s^2 y(s) + k_a(y(s) - x(s)) + b(sy(s) - sx(s)) = 0 \quad (2.20)$$

$$y(s)[m_a s^2 + k_a + bs] = x(s)[k_a + bs] \quad (2.21)$$

The rearranged form, with $y(s)$ isolated, is as follows:

$$y(s) = \frac{x(s)[k_a + bs]}{m_a s^2 + k_a + bs} \quad (2.22)$$

The Laplace transform of the equation 2.6 takes the following form:

$$m_t s^2 x(s) + k_a(x(s) - y(s)) + b(sx(s) - sy(s)) = k_t(U(s) - x(s)) \quad (2.23)$$

Rearranged form:

$$(m_t s^2 + k_a + bs + k_t)x(s) - (k_a + bs)y(s) = k_t U(s) \quad (2.24)$$

When $y(s)$ is substituted from the equation 2.21 and the formula is rearranged, the transfer function is written as follows:

$$(m_t s^2 + k_a + bs + k_t)x(s) - \frac{(k_a + bs)x(s)(k_a + bs)}{m_a s^2 + k_a + bs} = k_t U(s) \quad (2.25)$$

$$\frac{x(s)}{U(s)} = \frac{k_t(m_a s^2 + ka + bs)}{m_a m_t s^4 + b(m_a + m_t)s^3 + [k_t(m_a + m_t) + k_t m_a]s^2 + b k_t s + k_a k_t} \quad (2.26)$$

Rearranging the equations 2.21 and 2.25:

$$\begin{aligned} & \frac{k_t(m_a s^2 + ka + bs) \times U(s)}{m_a m_t s^4 + b(m_a + m_t)s^3 + [k_t(m_a + m_t) + k_t m_a]s^2 + b k_t s + k_a k_t} \\ &= \frac{y(s)(m_a s^2 + ka + bs)}{k_a + bs} \end{aligned} \quad (2.27)$$

Then substituted above equation and finding the transfer function for the sprung mass displacement:

$$\frac{y(s)}{U(s)} = \frac{bk_t s + k_a k_t}{m_a m_t s^4 + b(m_a + m_t)s^3 + [k_t(m_a + m_t) + k_t m_a]s^2 + bk_t s + k_a k_t} \quad (2.28)$$

Following the definition of the transfer functions, a corresponding model was developed in Simulink.

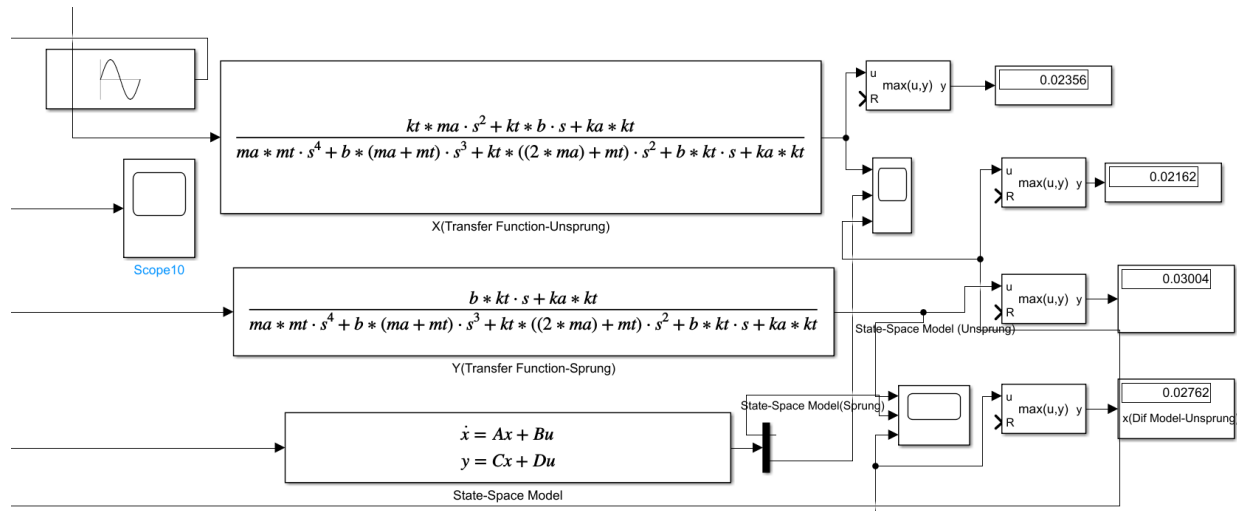


Figure 2.9:Simulink Model Transfer Function Model

The primary purpose of constructing this model was to perform verification and ensure consistency in the displacements of the sprung and unsprung components. Since the defined transfer functions specifically represent displacement behavior, acceleration and velocity were not further analyzed within this model. The transfer function model, similar to the differential and state-space models, was also driven by the same sine sinewave input, and the resulting displacements were subsequently compared. As a result, the transfer function model provides a representation that captures the fundamental dynamic characteristics of the system and yields results consistent with other modeling approaches. The agreement observed in the input-output responses supports the validity of the mathematical method employed.

3. OPTIMIZATION USING DOE

In today's automotive technologies, passenger comfort and vehicle stability are directly dependent on suspension system performance. Therefore, accurate determination and improvement of suspension parameters are critically important for both driving safety and comfort. This section provides a detailed explanation of the optimization process and the Design of Experiments (DOE) method employed.

Within the optimization scope, the goal was to test specific suspension parameters at various levels and analyze system responses corresponding to these combinations. The Design of Experiments method allowed these analyses to be performed systematically and efficiently. The applications were conducted using Minitab software, which facilitated both the generation of the experimental matrix and the execution of statistical analyses.

3.1 The Definition and Aim of Optimization

Optimization is the process of systematically adjusting parameters to ensure that a system performs optimally according to specific objectives. In engineering applications, particularly in cases where numerous variables influence system performance, optimization studies are widely used to enhance the efficiency and effectiveness of the system.

The criterion with respect to which the design is optimized, when expressed as a function of the design variables, is known as the criterion or merit or objective function. The choice of objective function is governed by the nature of problem. Thus the choice of the objective function appears to be straightforward in most design problems. However, there may be cases where the optimization with respect to a particular criterion may lead to results that may not be satisfactory with respect to another criterion. [24]

In this study, the aim of the optimization is to adjust the parameters of a vehicle's suspension system to achieve the most suitable values based on specific comfort and stability criteria. Comfort is associated with minimizing the vibrations felt by passengers during travel. Stability, on the other hand, relates to maintaining the vehicle's contact with the road and ensuring balanced driving behavior. Achieving a balance between these two objectives contributes to providing a safe and comfortable driving experience for both the driver and passengers. Parameters such as spring stiffness, tire stiffness and damping coefficient in the suspension system are critical variables that

directly affect these two performance metrics. Therefore, in this study, it is aimed to test these parameters at various levels, analyze the system responses, and determine the ideal parameter combinations.

3.1.1 Performance Metrics Considered in DOE

In the context of the DOE process, three key performance outputs were selected as the primary optimization targets: the tire-road contact force peak values, RMS of the body acceleration and the tire-road contact force. These metrics were used to quantitatively assess the effects of suspension parameter variations on both ride comfort and vehicle stability.

The **RMS of Body Acceleration** reflects the vertical vibration level experienced by the vehicle body. Lower RMS values indicate improved passenger comfort by reducing the transmission of road-induced vibrations to the occupants, especially over long driving periods.

The **Tire-Road Contact Force** represents the interaction force between the tires and the road surface. The continuity and stability of this force directly influence the vehicle's road holding capability and dynamic stability. Large fluctuations or reductions in the contact force can lead to decreased driving safety and control.

To evaluate and optimize this interaction, an objective function was formulated based on the RMS and peak-to-peak values of the tire-road contact force. The RMS value provides a measure of the overall energy and average force transmitted through the tire-road interface, reflecting how consistently the tire maintains contact with the road. A higher RMS value generally indicates better traction and stability.

However, the peak-to-peak value, which measures the difference between the maximum and minimum forces over time, captures the force fluctuations or oscillations. Large peak-to-peak variations imply instability and intermittent loss of contact, which negatively affect vehicle handling and ride comfort.

Therefore, the objective function aims to **maximize the RMS value** to ensure strong and continuous contact force, while simultaneously **minimizing the peak-to-peak value** to reduce force fluctuations and enhance stability. This balance promotes improved road-holding capability and driving safety by maintaining steady and reliable tire-road interaction.

Mathematically, the objective function to be minimized is defined as follows:

$$J = \frac{\text{peak to peak}(F_t)}{\text{RMS } F_t} \quad (2.29)$$

Minimizing J leads to a tire-road contact force profile that is both strong (high RMS) and stable (low peak to peak), achieving the desired performance in vehicle dynamics.

Three design parameters, considered as factors within the DOE process, were systematically varied to analyze their influence on the selected performance metrics:

- **Spring Stiffness:** Determines the vertical stiffness of the suspension system. Higher stiffness values generally improve stability but may compromise ride comfort.
- **Damping Coefficient:** Controls how rapidly the system dissipates vibrations. An appropriately tuned damping coefficient enhances body control and comfort.
- **Tire Stiffness:** Defines the tire's resistance to deformation. It directly impacts load transfer through the suspension and the behavior of the tire-road contact force, affecting both ride comfort and road holding.

These parameters were modeled at two different levels (low and high) and systematically analyzed using a DOE framework implemented in Minitab software. Based on the results, the system's performance was optimized by understanding how suspension tuning affects comfort and stability.

3.1.2 Optimization Approach Used

The objective of this study is to determine a parameter combination that improves both comfort and stability. Since comfort and stability often exhibit opposing tendencies, such problems are addressed within the scope of multi-objective optimization.

In order to efficiently investigate the effects of the parameters used in the optimization process and to keep the number of experiments under control, the DOE method was preferred. In this study, a 2^k full factorial experimental design was applied within the DOE framework. This structure allowed for all parameter combinations to be tested systematically. [25]

The 2^k full factorial design is an experimental planning method that includes all possible combinations of k factors, each defined at two levels. This method enables the analysis of not only

the individual effects of each factor but also the interactions between factors. As a result, a more comprehensive understanding of the system is achieved. Since three factors were used in this study, $2^3 = 8$ experimental combinations were created.

With the visual and statistical analysis tools provided by the Minitab software, the effects of each parameter on the system outputs were thoroughly evaluated, and this information was directly integrated into the optimization process. In this way, reliable and statistically significant results were obtained with far fewer simulations compared to traditional trial and error methods.

3.2 Design of Experiments (DOE) Application

Design of Experiments (DOE) is a method used to systematically and statistically analyze the effects of different factors within a system. DOE is employed in complex systems where multiple parameters change simultaneously, in order to identify which factors have significant effects on system performance. Compared to traditional single-parameter analyses, it provides more comprehensive information with fewer experiments.

In this study, the DOE method was chosen to analyze both the individual and combined effects of three key suspension system parameters (spring stiffness, damping coefficient, and tire stiffness). Investigating the parameters at different levels enabled the observation of changes in performance outputs and the identification of optimal conditions.

3.2.1 Design of Experiment: Factors, Levels, and Method Selection

In this study, three main control factors were determined during the experimental design process: spring stiffness, damping coefficient, and tire stiffness.

For each factor, two levels were defined: a **low level** and a **high level**. These levels were determined considering engineering justifications and the physical limits of the suspension system. This allowed for an analysis of how the system responds to soft and stiff parameters.

C5	C6	C7	C8	C9	C10	C11
Spring Stiffness	Damping Coefficient	Tire Stiffness	RMS Body Acceleration	Tire Contact Force Peak to Peak	Tire Contact Force RMS	J
16000	1000	150000	1,2550	1014,0	343,3	2,95
22000	1000	150000	1,0640	1026,0	297,1	3,45
22000	1000	220000	1,0190	969,2	284,7	3,40
16000	3000	150000	0,7641	751,6	219,7	3,42
16000	3000	220000	0,7413	813,3	213,1	3,82
16000	1000	220000	1,1990	969,6	328,0	2,96
22000	3000	150000	0,7967	785,5	228,9	3,43
22000	3000	220000	0,7712	839,0	221,6	3,79

Figure 3.1:Experiment Matrix and Simulation Output

Here in this table RMS body acceleration values are in $[m/s^2]$, tire-road contact forces and their RMS values are in $[N]$.

3.2.2 Analysis

Each experimental combination was simulated using the suspension model developed in the MATLAB/Simulink environment. The resulting performance outputs, RMS of body acceleration, RMS of the tire-road contact force and peak to peak force were transferred to Minitab and statistically analyzed.

Effect Analysis for RMS of Body Acceleration:

For the analysis of this criterion, Pareto charts generated by Minitab were utilized. The graphs showing the absolute effects and statistical significance levels of the factors are provided respectively.

The p-value is a statistical measure that helps determine whether the observed effects in a data set are statistically significant or occurred by chance. In the context of analysis of variance (ANOVA), it is used to assess the significance of each factor on the response variable. A low p-value indicates strong evidence that a factor has a real influence on the output.

Elimination is performed to remove factors that do not have a statistically significant impact on the system. This improves the clarity and efficiency of the model by focusing only on meaningful parameters. Lower p values give more evidence against the null hypothesis; when p values < 0.05 , it reveals that the factor impact is substantial and the null hypothesis may be rejected. [26]

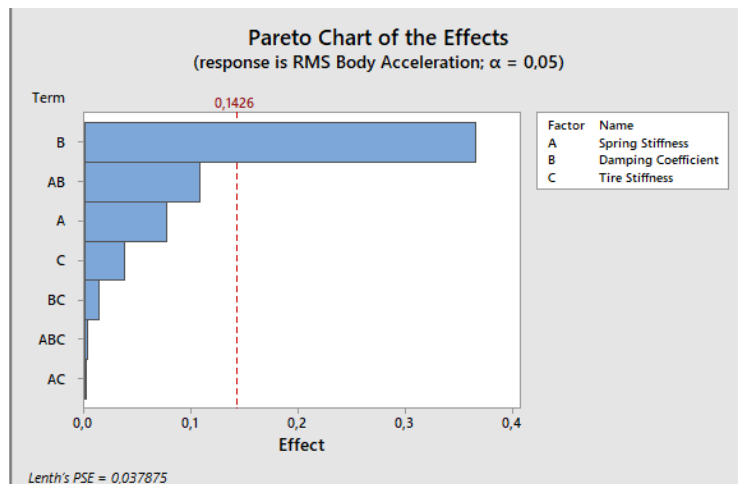


Figure 3.2:Pareto Graph for RMS of body acceleration

In Figure 3.2 clearly shows that the **damping coefficient (B)** has by far the greatest effect, followed by **spring stiffness (A)** and the **AB interaction**. Only **B** is above the significance limit of 0.1426 in terms of effect magnitude. For this reason firstly the interaction ABC should be eliminated.

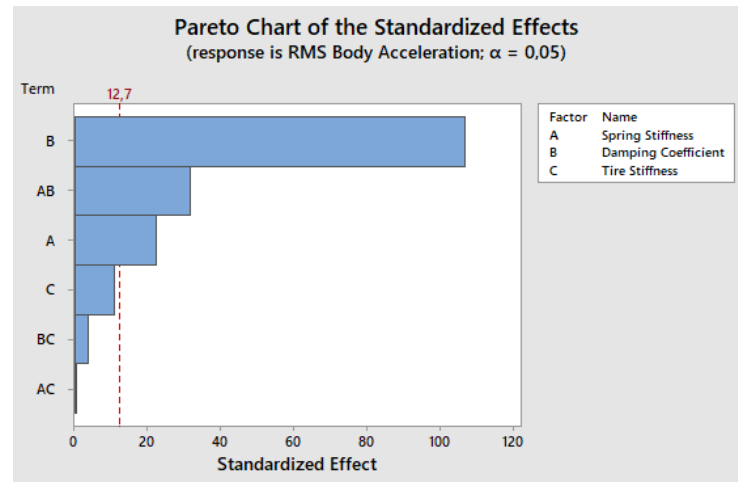


Figure 3.3: Pareto Chart after first iteration for RMS of Body Acceleration

In this Pareto chart, obtained after the first iteration, the **damping coefficient (B)** parameter clearly surpassed the 95% confidence limit, standing out as the only statistically significant factor influencing the performance criterion. While **spring stiffness (A)** and the **AB interaction** exhibited certain effects. Since the p-value of the some interaction is above 0.05, it will be removed from the model. Also, as there are still insignificant effects, the iteration will continue.

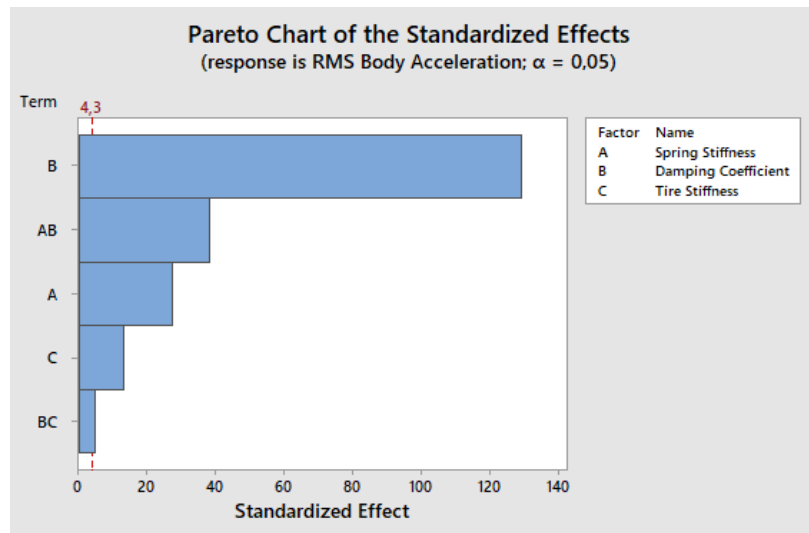


Figure 3.4:Pareto Chart after second iteration for RMS of Body Acceleration

Furthermore, the **AC interaction**, which had a very low impact in the first iteration, was removed from the model in the second iteration. This resulted in a simpler and more meaningful structure for the effect analysis. As illustrated in Figure 3.4, following the second iteration, several factors, spring stiffness (A), damping coefficient (B), tire stiffness (C), as well as the interaction terms AB and BC, exhibit standardized effect values that exceed the statistical significance threshold ($\alpha = 0.05$). This confirms that these parameters have a meaningful and statistically significant influence on the RMS value of body acceleration.

Effect Analysis for Tire-Road Contact Force (Peak to Peak Value)

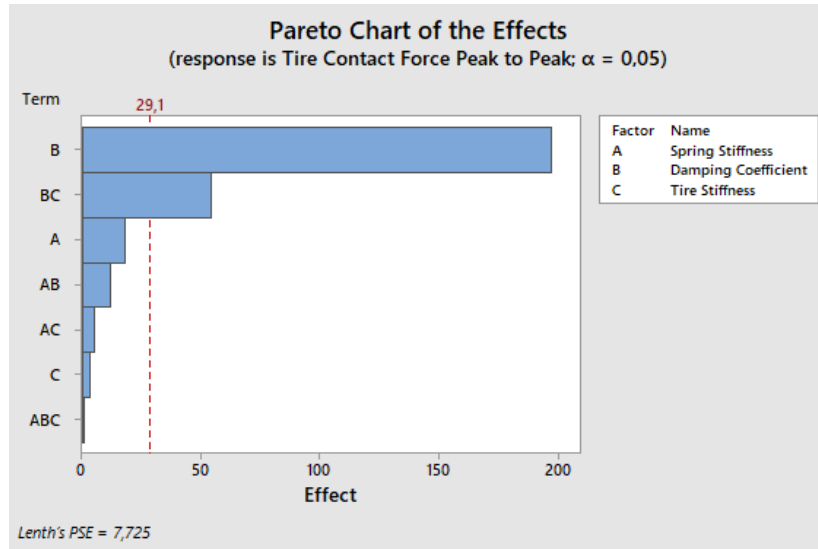


Figure 3.5:Pareto Graph Tire-Road Contact Force (peak to peak value)

Based on the Pareto charts, the damping coefficient (B) is the parameter with the highest and most significant effect on this performance output. B and BC interaction are the factors exceeding the significance limit.

In order to enhance model clarity and focus on statistically meaningful terms, the removal of insignificant factors becomes essential. Therefore, the ABC interaction, having the lowest standardized effect below the significance threshold, should be the first to be eliminated.

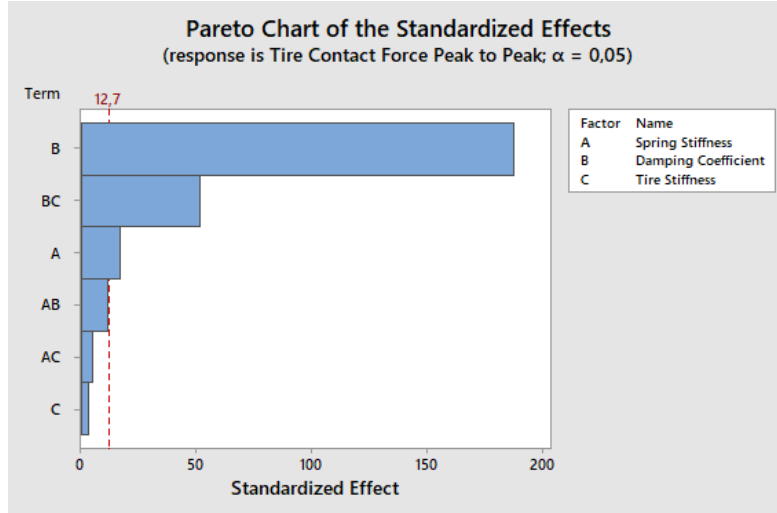


Figure 3.6. Pareto Chart of after first iteration for Tire-Road Contact Force (peak to peak value)

The damping coefficient (B) emerged as by far the most dominant factor, exhibiting a very high standardized effect. Additionally, the BC interaction term and the spring stiffness (A) both exceeded the statistical significance threshold of 12.7. Next, the AC interaction term, which did not meet the significance threshold, will be eliminated in the subsequent step.

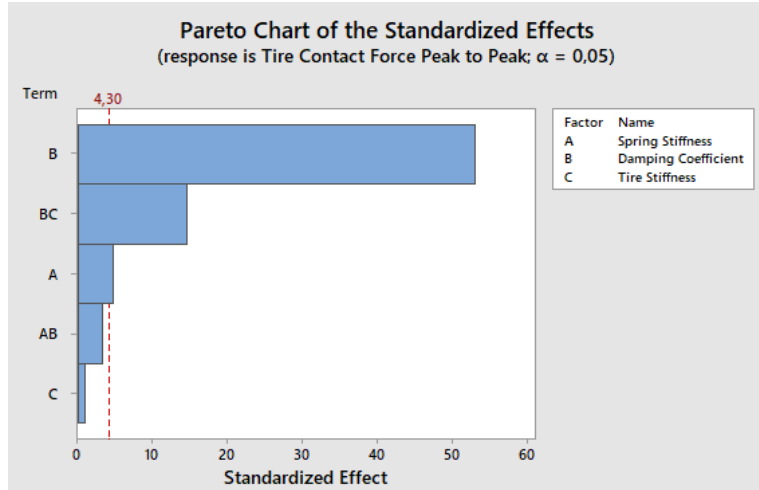


Figure 3.7:Pareto Chart of after second iteration for Tire-Road Contact Force (peak to peak)

This second iteration model, which was created after the first iteration by removing ineffective interaction term AC from the model.

Analysis of Variance

Source	DF	Adj SS	Adj MS	F-Value	P-Value
Model	4	84405,8	21101,5	184,43	0,001
Linear	3	78552,2	26184,1	228,85	0,000
Spring Stiffness	1	633,7	633,7	5,54	0,100
Damping Coefficient	1	77894,0	77894,0	680,79	0,000
Tire Stiffness	1	24,5	24,5	0,21	0,675
2-Way Interactions	1	5853,6	5853,6	51,16	0,006
Damping Coefficient*Tire Stiffness	1	5853,6	5853,6	51,16	0,006
Error	3	343,3	114,4		
Total	7	84749,1			

Figure 3.8 Analysis of Variance Results for Tire Road Contact Force (Peak to Peak)

As shown in the figure 3.8, the p-value for the C parameter is above the significance threshold. However, since it is a fundamental parameter, it cannot be eliminated. At this point, the Pareto analysis for the tire-road contact force peak-to-peak value concludes. As a result, it is observed that the most influential parameters are B, BC, and A.

Effect Analysis for RMS of the Tire-Road Contact Force

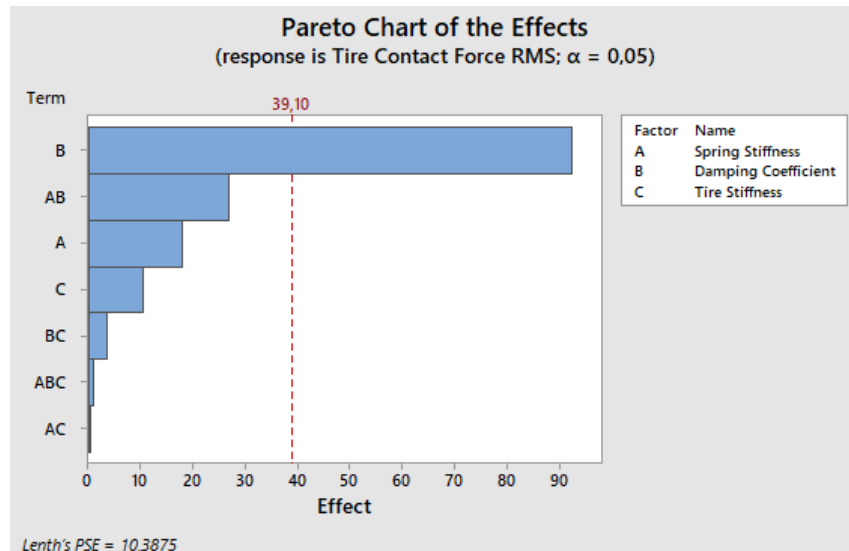


Figure 3.9 Pareto Graph Tire-Road Contact Force (RMS)

Based on the figure 3.9, the damping coefficient (B) is the parameter with the highest and most significant effect on this performance output.

The first step should be to eliminate the ABC interaction, which, having the lowest standardized effect below the significance threshold, should be the first to be eliminated.

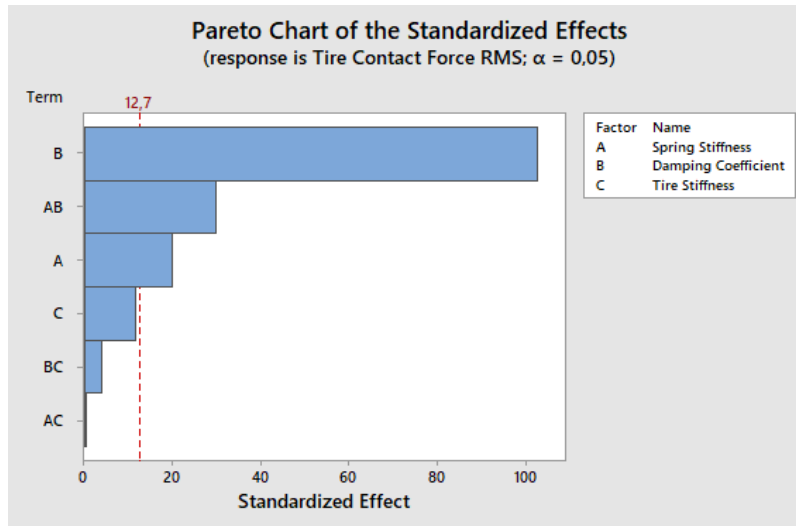


Figure 3.10 After ABC eliminated for Tire-Road Contact Force (RMS)

Based on the Pareto chart analysis, the next term to be eliminated should be the AC interaction.

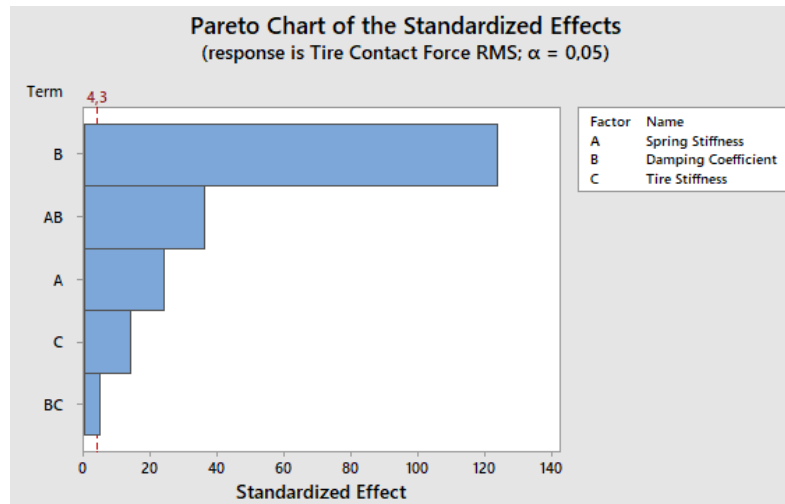


Figure 3.11 After AC eliminated for Tire-Road Contact Force (RMS)

The final Pareto Chart obtained after the elimination steps is presented in Figure 3.11. In this final analysis, the damping coefficient (B) stands out as the most dominant factor, having the most significant impact on the system response. The AB interaction term and the spring stiffness (A) also remain above the statistical significance threshold (4.3), maintaining their meaningful influence on the system.

The effects of the other factors are likewise above the significance threshold, indicating that no further elimination is necessary in the model.

These results confirm that unnecessary terms have been successfully removed, resulting in a simplified yet highly explanatory model. Consequently, through these iterations, the most critical parameters have been identified, and the goal of model simplification has been achieved. This provides a solid foundation for future designs aimed at improving the vehicle's suspension performance

Analysis of Variance

Source	DF	Adj SS	Adj MS	F-Value	P-Value
Model	5	19415,0	3883,0	3490,34	0,000
Linear	3	17954,7	5984,9	5379,69	0,000
Spring Stiffness	1	644,4	644,4	579,24	0,002
Damping Coefficient	1	17094,0	17094,0	15365,40	0,000
Tire Stiffness	1	216,3	216,3	194,44	0,005
2-Way Interactions	2	1460,3	730,1	656,31	0,002
Spring Stiffness*Damping Coefficient	1	1436,5	1436,5	1291,22	0,001
Damping Coefficient*Tire Stiffness	1	23,8	23,8	21,40	0,044
Error	2	2,2	1,1		
Total	7	19417,2			

Figure 3.12 Analysis of Variance Results for Tire Road Contact Force (RMS)

As shown in the figure 3.12, the p-value for all parameters are below the 0.05. At this point, the Pareto analysis for the tire-road contact force RMS value concludes. As a result, it is observed that the most influential parameters are B, AB, and A.

3.2.3 Effect of DOE Results on Optimization

DOE analysis identified the damping coefficient as the most influential parameter affecting all performance criteria: the RMS value of body acceleration, the RMS value of the tire-road contact force, and the peak-to-peak value of the tire-road contact force. The damping coefficient demonstrated high statistical significance across all outputs, playing a decisive role in the optimization process.

In contrast, other parameters such as spring stiffness and tire stiffness exhibited secondary effects, which were not substantial enough to induce significant changes in the system response. Consequently, the damping coefficient was validated as a highly effective and impactful variable in the optimization of suspension performance.

Although the tire-road contact force is generally modeled through the tire stiffness coefficient, in practice, the damping effect plays a much more critical role in the dynamic behavior of this force as shown in figure 3.11. Stiffness represents the elastic response of the tire against the road surface, while damping determines how the tire dissipates energy during motion. When the tire encounters irregularities on the road, the resulting vibrations and shocks are balanced not only by elastic deformation but also by damping forces. Therefore, to accurately model the dynamic behavior of the contact force, the effect of the damping coefficient is more dominant than that of the stiffness. Damping affects the magnitude and duration of force fluctuations by controlling the energy exchange between the tire and the road; thus, it plays a more significant role in the overall magnitude and characteristics of the tire-road contact force.

The application of the DOE methodology enabled a reduction in the number of experimental runs without compromising the reliability or informativeness of the results. Based on the optimal parameter combinations identified through the analysis, the suspension system achieved a balanced performance in terms of both ride comfort and road-holding stability.

4. RESULTS AND DISCUSSION

This section presents the findings from the simulation and DOE studies conducted on the quarter-car suspension system model. First, the mathematical and physical models were compared as part of the system validation efforts. Next, the effects of parameter variations on system responses were analyzed. Finally, within the scope of the DOE and optimization process, the performance outputs of different scenarios were evaluated, and the optimum parameter combination was determined.

4.1 Model Verification Results

The mathematical model of the quarter-car suspension system developed in this study was structured in the Simulink environment in both differential model, state-space, and transfer function forms. To test the model accuracy, the same road input was applied to each model, and the system responses were compared.

The comparison was checked based on the displacement of the sprung and unsprung masses. The obtained results indicate that the state-space and transfer function models yielded highly consistent results.

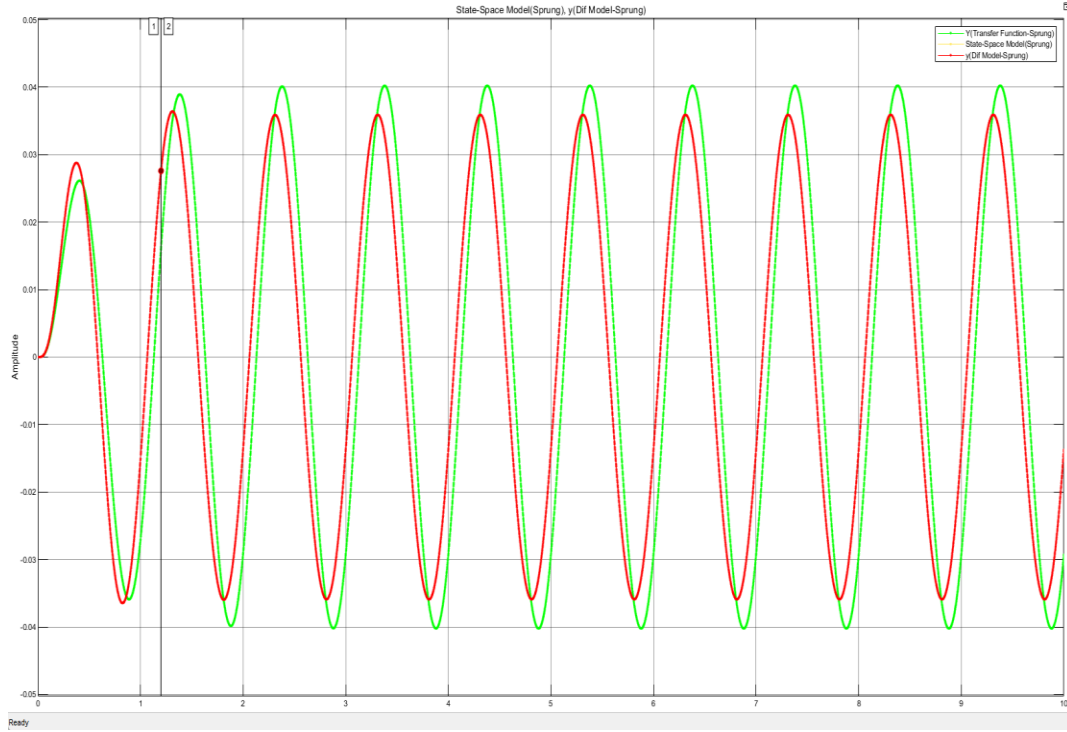


Figure 4.1: Sprung Displacements Graph

In figure 4.1, the displacement graphs of the sprung mass for all three models are presented in an overlaid manner. As can be seen, the green line represents the transfer function graph. The red line graph, on the other hand, shows the differential equation model. Additionally, the state-space model, which coincides with this differential model, will be the yellow line graph. While perfect overlapping was achieved for the differential equation and state-space models, a deviation from these two was observed in the transfer function model.

These displacement graphs are also provided separately below. Looking at the section on the right side of the graph where the measurements are located, the amplitude values of the differential

model and state-space models at 1.2 seconds are the same. As a result of our observations here, we assumed that verification was provided.

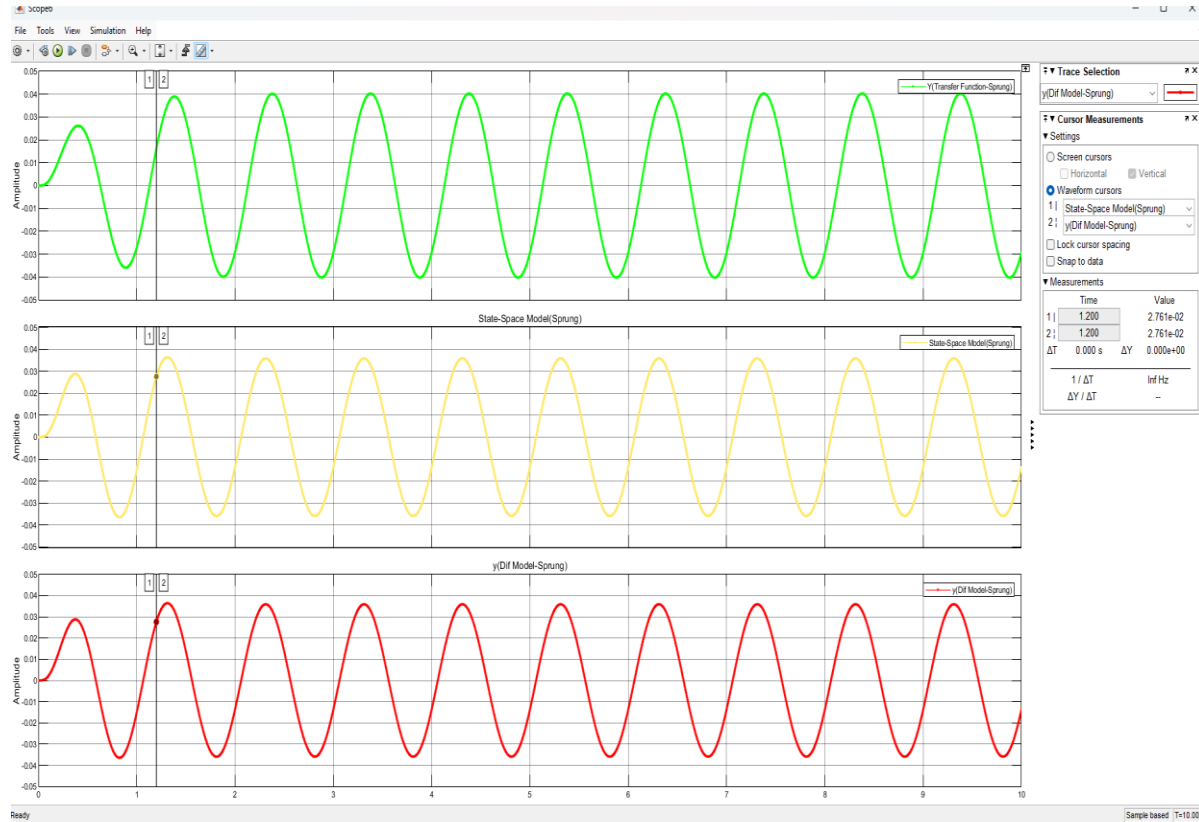


Figure 4.2:Sprung Displacements Graphs

Similarly, the displacement graph for the unsprung mass for all three models is provided below, shown in coincident form. Looking at the measurements here, too, the state-space and differential model measurements coincide with each other. However, different values are still read for the transfer function-based model.

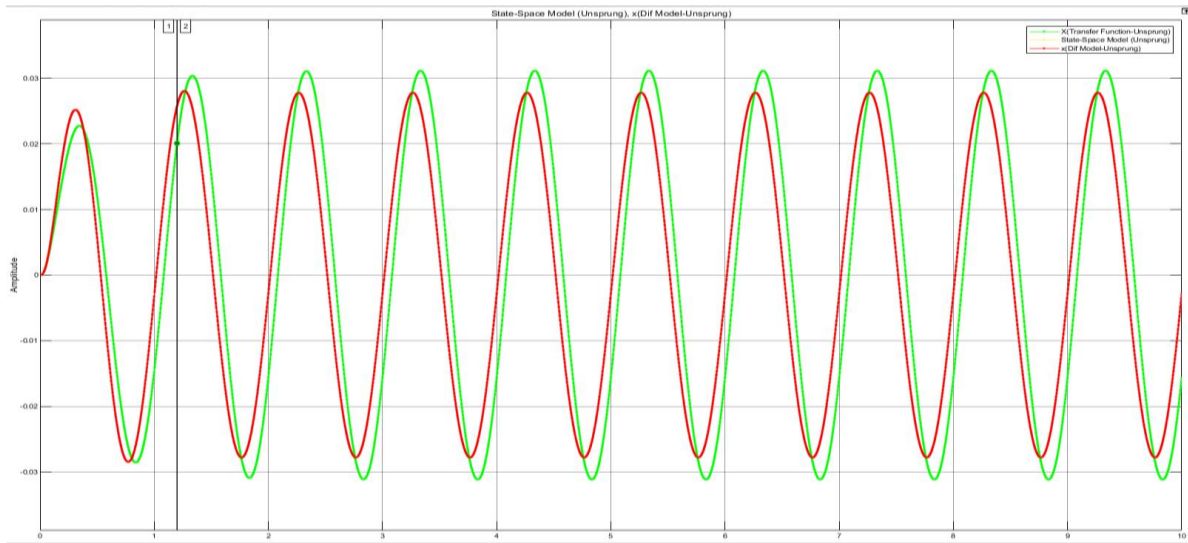


Figure 4.3: Unsprung Displacements Graphic

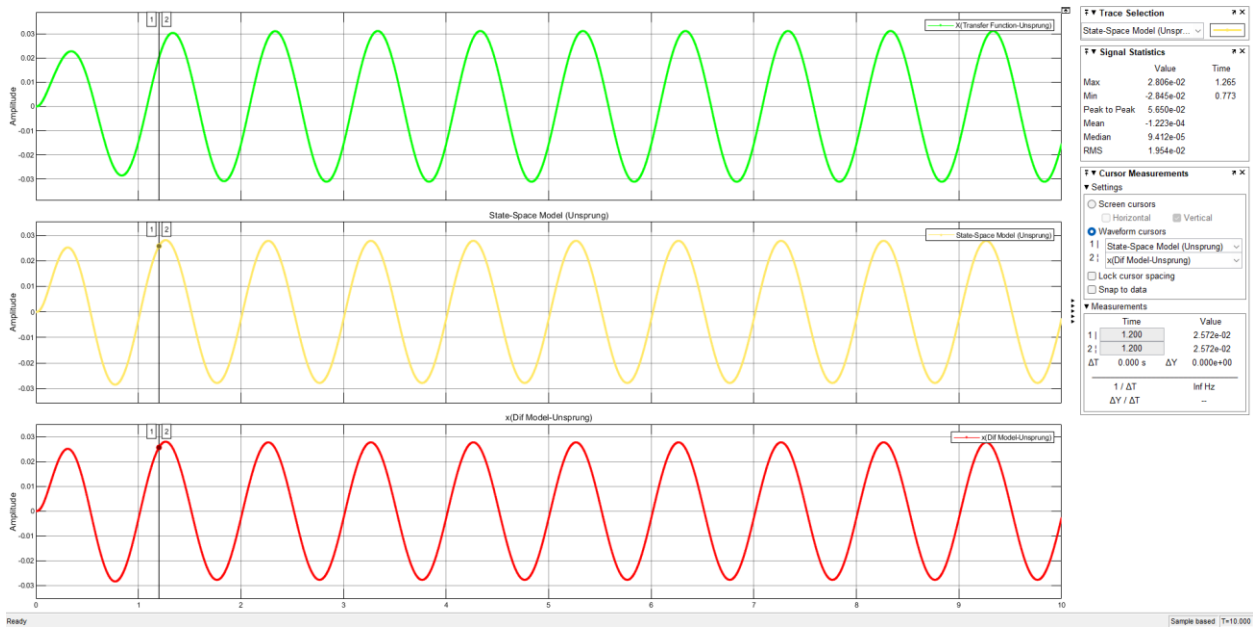


Figure 4.4: Unsprung Displacements Graphics

As seen in the figure 4.4, verification for both the state-space and differential models was provided based on measurements taken at the 1.2-second mark.

TF models describe only the input-output relationship of a system and do not explicitly include internal state variables. As a result, TF models provide a limited representation of the system's dynamic behavior, particularly during the transient response phase. In contrast, differential

equation and state-space models incorporate internal state variables that represent the physical properties of the system—such as mass, damping, and inertia—allowing for a more accurate depiction of the system's behavior over time. Especially in response to sudden input changes or rapidly varying signals, TF models tend to produce an idealized and simplified output, whereas state-space and differential models yield transient responses that are more consistent with physical reality. Therefore, even under ideal conditions where initial states and numerical solvers are aligned, minor yet systematic deviations can occur in TF model outputs. These deviations are primarily attributed to the transfer function's inability to explicitly represent the internal dynamics of the system. Consequently, it is likely that the observed deviation originates from this limitation.

4.2 Parameter Effect Analysis

Three key parameters affecting the performance of the quarter-car suspension system have been identified:

- Spring constant
- Damping coefficient
- Tire stiffness

Changes in system responses were analyzed by applying these parameters at different levels. The following fundamental performance metrics were used:

- Sprung mass acceleration RMS value
- Tire-road contact force peak to peak value
- Tire-road contact force RMS value

4.2.1 Effects of Spring Stiffness

Graphs were generated using the determined lower and upper parameters to examine the effect of spring stiffness on the suspension system.

Below is the graph showing the sprung mass acceleration when the spring stiffness is varied, while the damping coefficient and tire stiffness are kept at their average values.

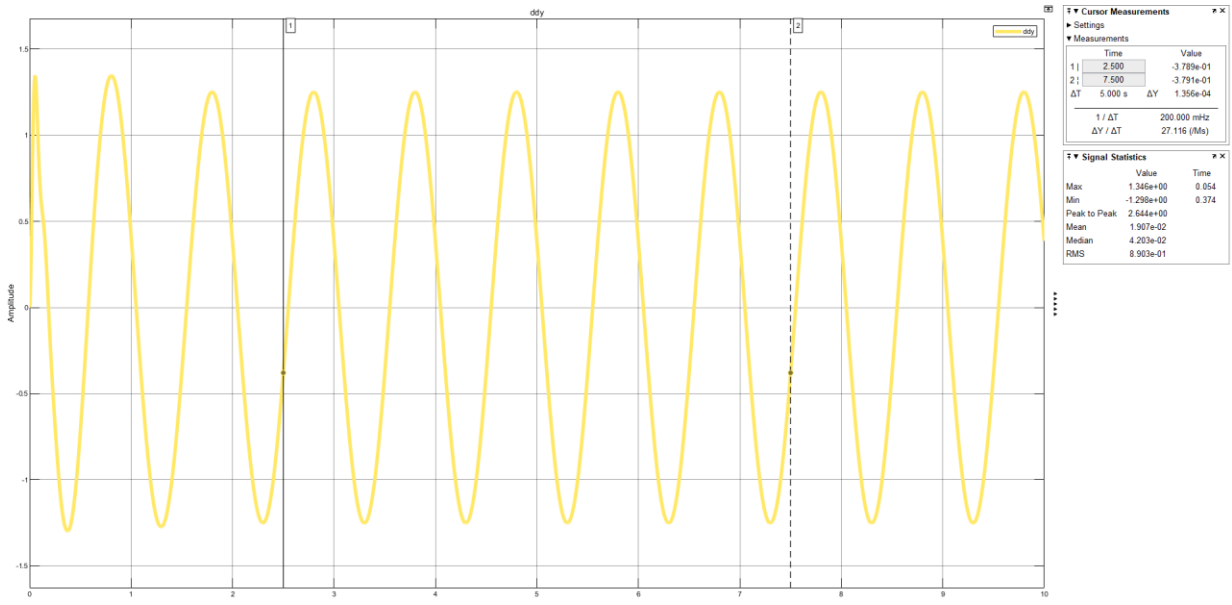


Figure 4.5: Sprung Acceleration Graphic for Spring Stiffness =22000N/m

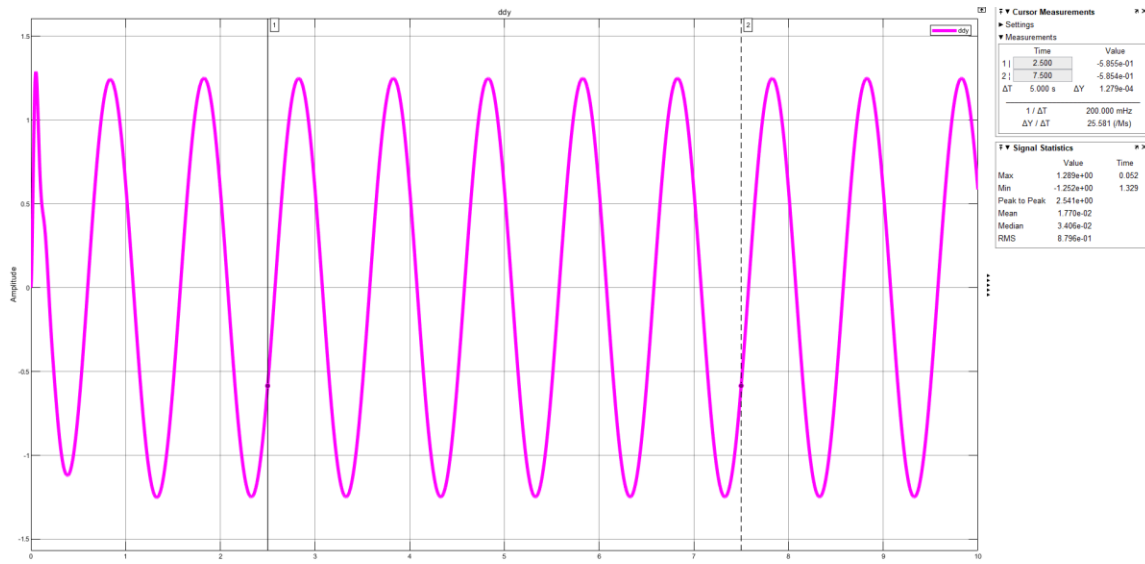


Figure 4.6: Sprung Acceleration Graphic for Spring Stiffness=16000N/m

In these two graphs, the tire stiffness is set to 185000 N/m, and the damping coefficient is 2000Ns/m. The spring stiffness, on the other hand, is 16000 N/m in the first graph, while it is 22000N/m in the other. As a result, when the spring is soft, the maximum acceleration is 1.289 m/s². However, when we increase the spring stiffness to 22000 N/m, we observe that this maximum acceleration rises to 1.346 m/s².

An increase in the sprung mass acceleration response was observed when the spring stiffness was increased. A stiffer spring caused the system to oscillate more at a higher frequency. An increase in RMS values from 0.8796 m/s to 0.8923 m/s was observed. Consequently, the increase in spring stiffness in this model increased the RMS value, which negatively affected ride comfort.

4.2.2 Effects of Damping Coefficient

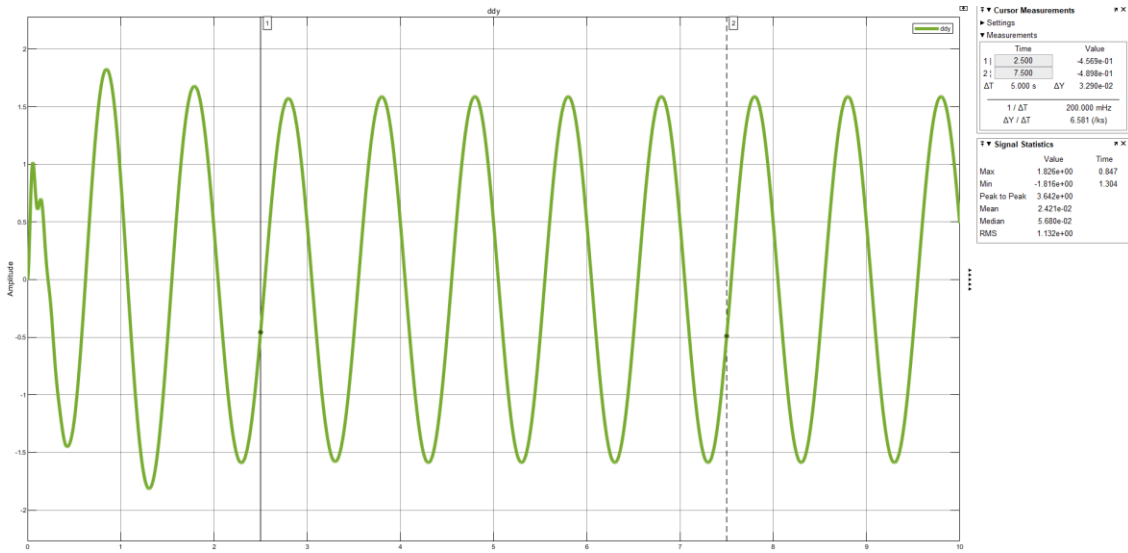


Figure 4.7:Sprung mass acceleration for Damping Coefficient of 1000 Ns/m

In this sprung mass acceleration graph, the damping coefficient was set to its lower limit of 1000 Ns/m. The parameters k_a and k_t in the model were taken as their average values, 19000 N/m and 185000 N/m, respectively.

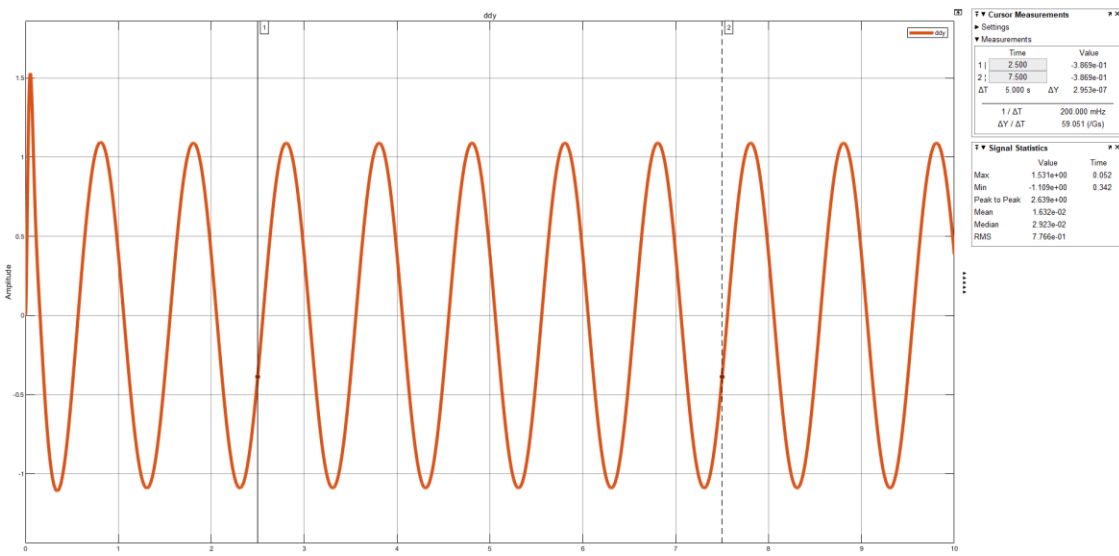


Figure 4.8:Sprung Mass Acceleration for Damping Coefficient of 3000 Ns/m

In this graph, as the damping coefficient increases from 1000 to 3000 Ns/m, other parameters are kept constant.

As a result of the simulations, a significant decrease in the sprung mass acceleration was observed with an increase in the damping coefficient. This finding is consistent with control systems theory, demonstrating that increased damping leads to faster stabilization of system oscillations, thereby enhancing passenger comfort.

Numerically speaking, increasing the damping coefficient significantly reduced the sprung mass acceleration RMS value. This decrease proves that vibration energy is dissipated more efficiently with increased damping, and consequently, vibrations are damped more quickly and effectively. These findings clearly indicate that optimal damping settings play a critical role in passenger comfort in vehicle suspension systems.

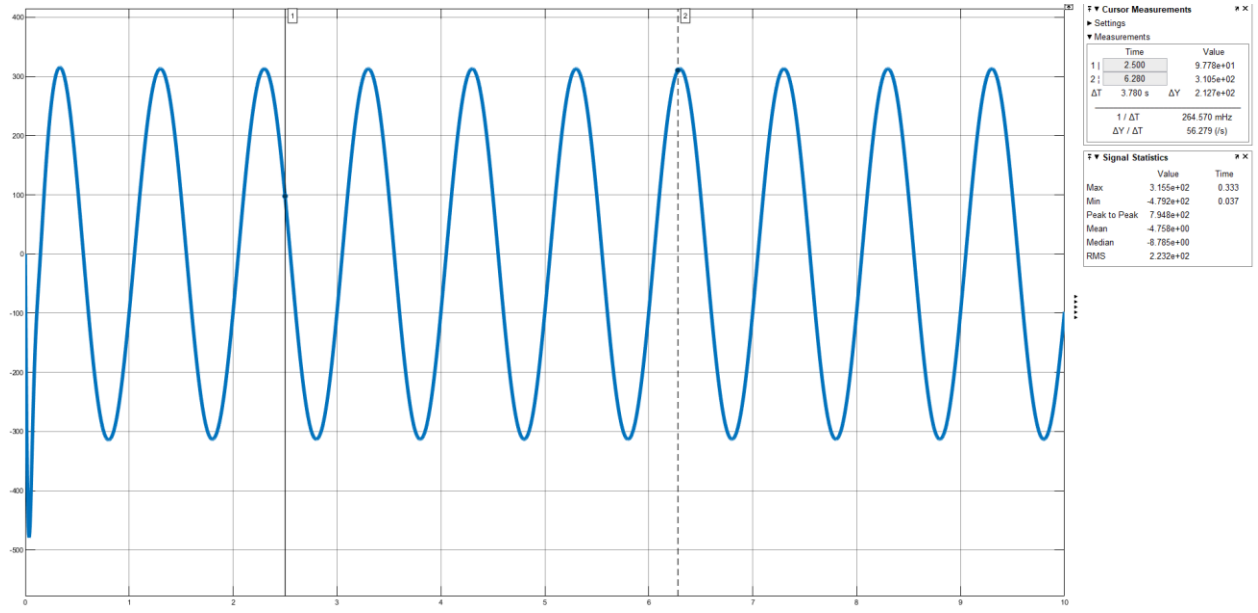


Figure 4.9:Tire-Road Contact Force for Damping stiffness is equal to 3000 Ns/m

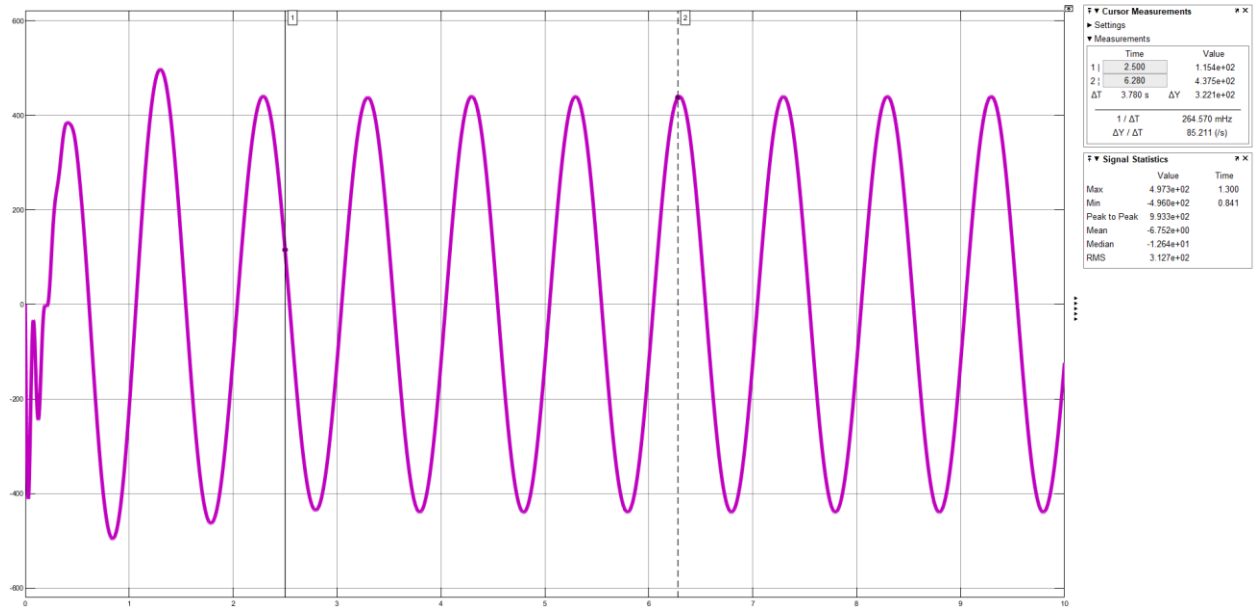


Figure 4.10:Tire-Road Contact Force for Damping Coefficient of 1000 Ns/m

When examining the effect of the damping coefficient on the tire-road contact force, a significant reduction in the dynamic variations of this force was observed with an increase in the damping coefficient. When the damping coefficient was reduced from 3000 Ns/m to 1000 Ns/m, a increase was recorded in both the maximum values (from 497.3 N to 315.5 N) and the peak-to-peak values

(from 794.8 N to 933.3 N) of the tire-road contact force. Most notably, the RMS tire-road contact force value increased from 222.2 N to 312.7 N.

Increasing the damping coefficient reduces the peak tire-road contact force, but this effect contributes positively to road holding. A higher damping level helps to suppress excessive oscillations in the contact force, resulting in a more stable and continuous tire-road interaction. This stability is essential for maintaining consistent road grip and improving vehicle handling. In contrast, lower damping results in larger force peaks and greater fluctuations, which can compromise road holding and lead to less predictable vehicle behavior.

4.2.3 Effects of Tire Stiffness

In this section, the effects of tire stiffness on both the body acceleration response and the tire-road contact force are analyzed. While increasing tire stiffness has a relatively limited impact on the body acceleration response, it produces a more pronounced effect on the tire-road contact force. Higher tire stiffness improves road holding capability but also transmits higher-frequency road forces into the suspension system, which may negatively affect ride comfort. The following analysis explores these interactions in detail.

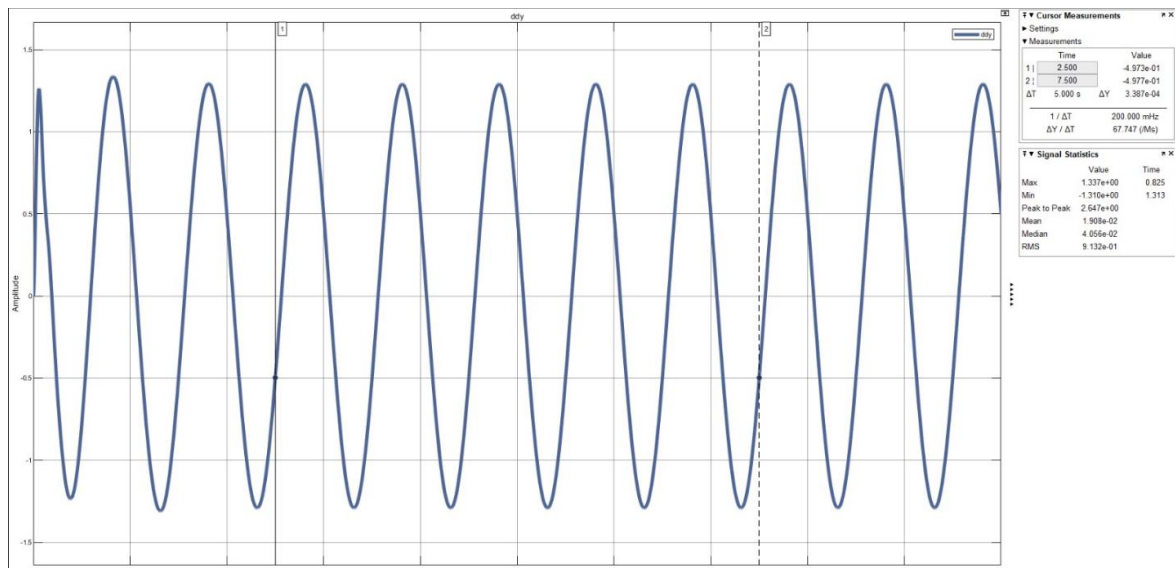


Figure 4.11: Sprung Mass Acceleration for Tire Stiffness of 150000 N/m

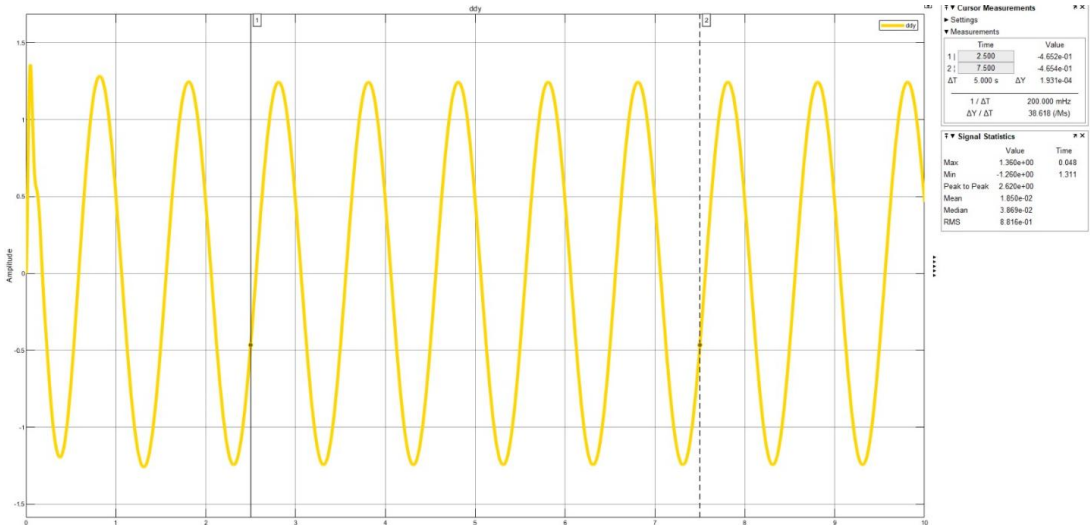
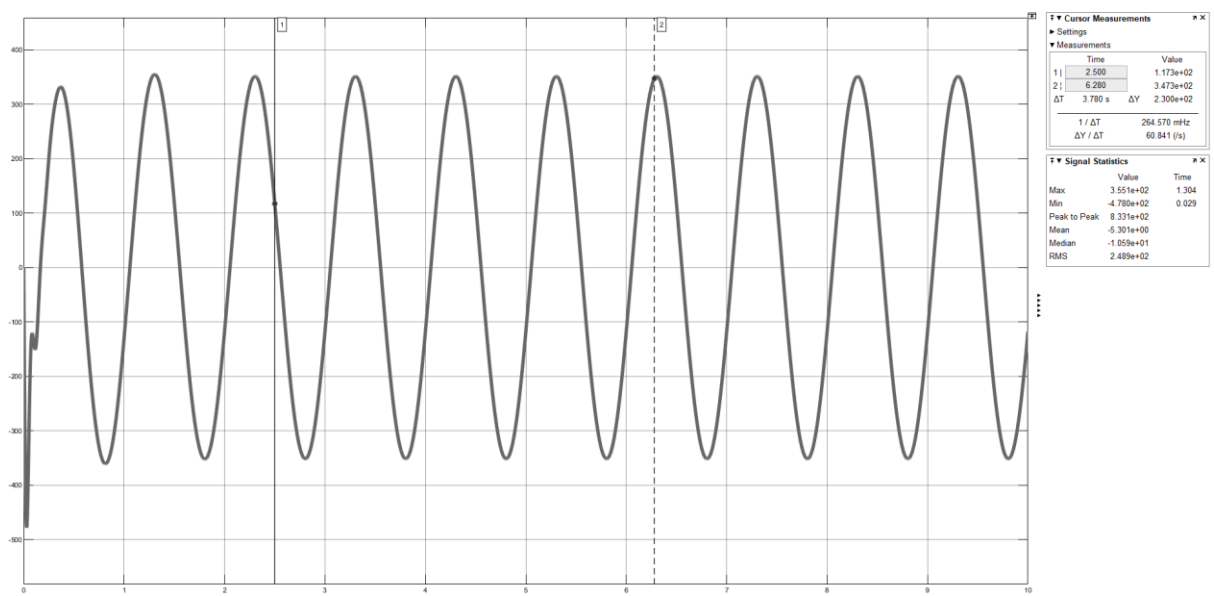
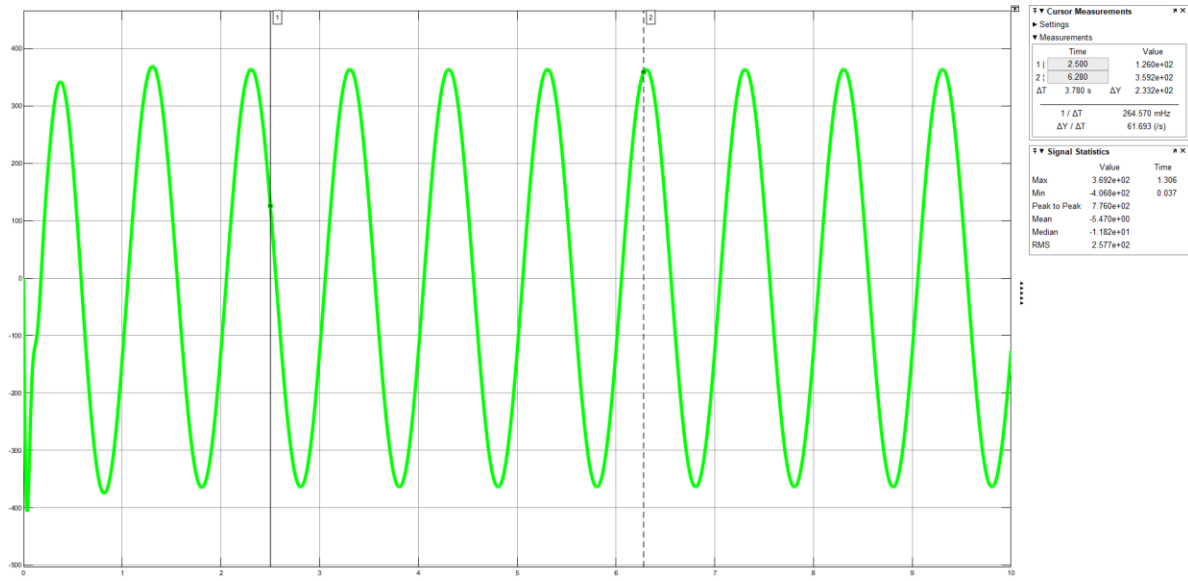


Figure 4.12: Sprung Mass Acceleration for Tire Stiffness of 220000 N/m

As shown in Figures 4.11 and 4.12 that increasing the tire stiffness has a limited effect on the body acceleration response. In figures, the RMS and peak-to-peak values of the body acceleration remained largely unchanged across the tested tire stiffness levels. This indicates that tire stiffness mainly influences the tire-road contact force, while its impact on ride comfort, represented by body acceleration, is relatively minor.

The results presented in Figures 4.13 and 4.14 demonstrate that increasing the tire stiffness from 150000 N/m to 220000 N/m has a noticeable effect on the tire-road contact force. Specifically, the RMS value of the contact force increased, and the overall peak-to-peak amplitude became larger with higher tire stiffness. This indicates that a stiffer tire transmits more of the road surface irregularities into the suspension system, leading to higher fluctuations in the contact force. While this may improve road holding capability by reducing tire deformation under dynamic loads, it also results in greater force variations, which can negatively affect ride comfort and overall dynamic stability.



4.3 Design of Experiment and Optimization Results

To more effectively evaluate system performance, the DOE method was applied.

In the DOE study:

- Factors: Spring stiffness, damping coefficient, tire rigidity
- Factor Levels: Two levels for each (low, high)
- Number of Scenarios: 8 (full factorial design)

were established, and for each scenario, RMS body acceleration, peak to peak value of the tire-road contact force and RMS of the tire road contact force were measured.

Table 2: RMS and Tire Road Contact Force Results

Spring Stiffness [N/m]	Damping Coefficient [Ns/m]	Tire Stiffness [N/m]	RMS Body Acceleration [m/s ²]	Peak to Peak Value of the Tire Road Contact Force [N]	RMS of the Tire Road Contact Force [N]	Objective Funtion J
16000	1000	150000	1.2550	1014	343.3	2.95
22000	1000	150000	1.0640	1026	297.1	3.45
16000	3000	150000	0.7641	751.6	219.7	3.42
22000	3000	150000	0.7967	785.5	228.9	3.43
16000	1000	220000	1.1990	969.6	328	2.96
22000	1000	220000	1.0190	969.2	284.7	3.40
16000	3000	220000	0.7413	813.3	213.1	3.82
22000	3000	220000	0.7712	839	221.6	3.79

4.3.1 ANOVAMain Effect Plots

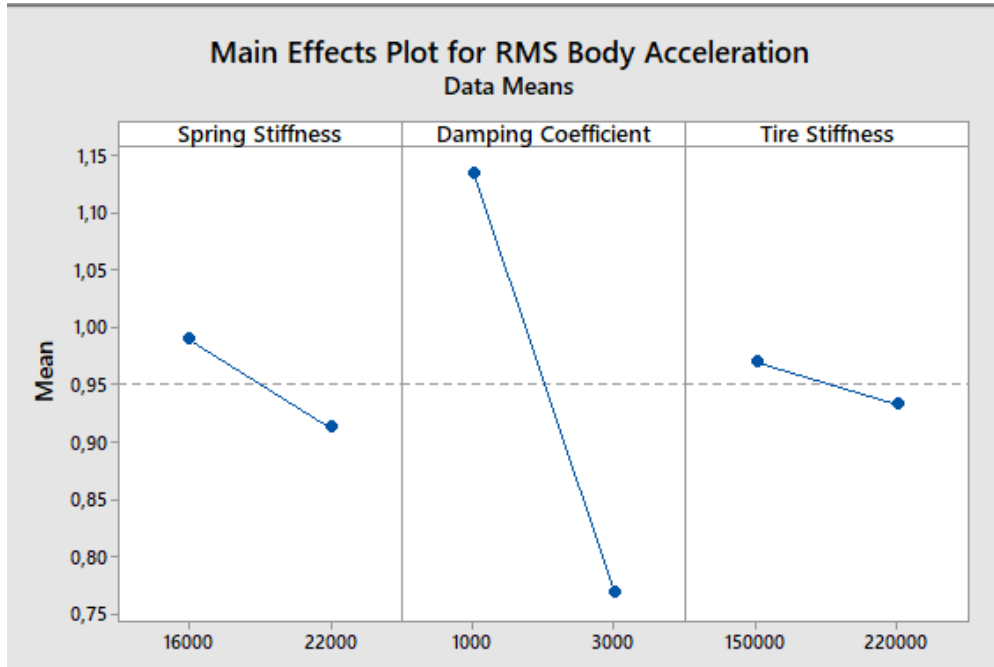


Figure 4.15: Main Effect Plot for Body Acceleration

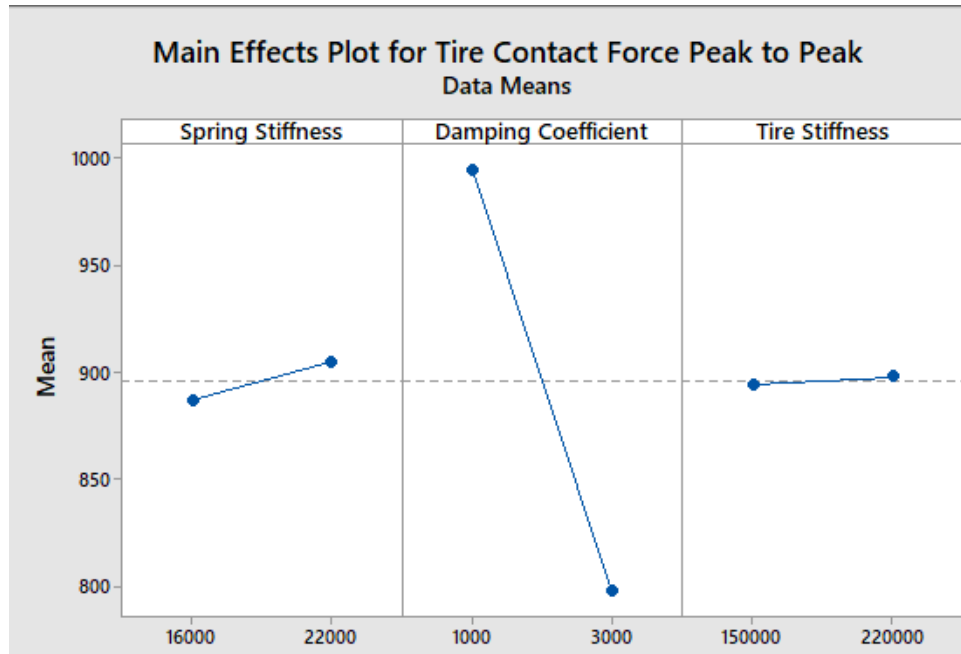


Figure 4.16: Main Effect Plot for Tire Contact Force Peak to Peak

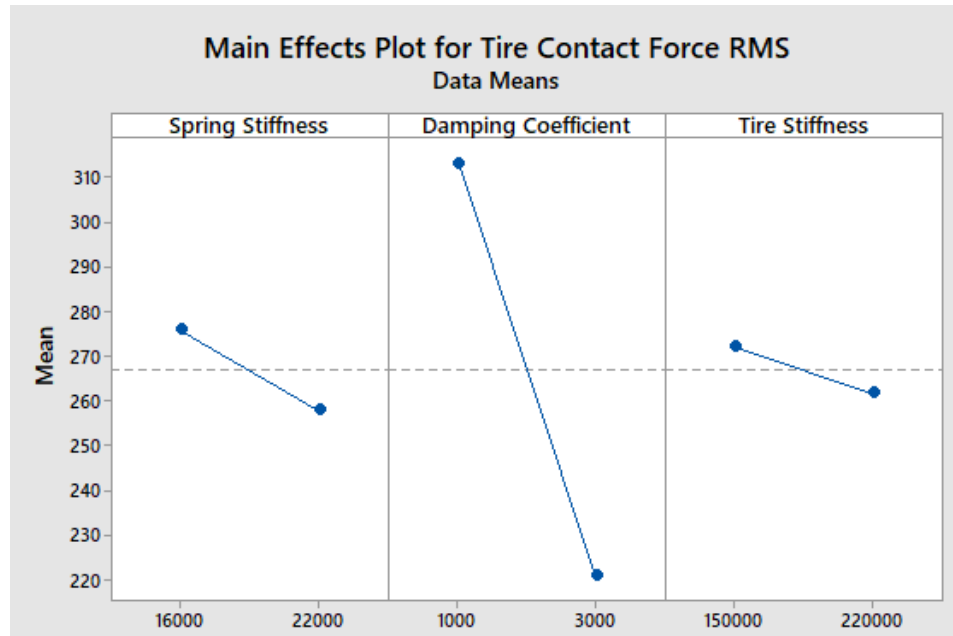


Figure 4.17: Main Effect Plot for Tire Contact RMS

The Main Effects Plots shown in the figures illustrate the individual impacts of suspension system design parameters—spring stiffness, damping coefficient, and tire stiffness—on three different performance outputs: RMS Body Acceleration, Tire Contact Force Peak to Peak, and Tire Contact Force RMS. Each plot presents the average values of the respective performance metric across different factor levels, enabling a comparative analysis. As clearly observed from the graphs, the damping coefficient has a significant effect on all performance measures; increasing the damping value reduces both body acceleration and fluctuations in the tire-road contact force, thereby contributing to a more stable ride. While the effects of spring and tire stiffness are more limited, they can still positively influence performance under certain parameter combinations. This analysis serves as a guide in identifying which parameters should be prioritized during the optimization process.

4.3.2 Response Optimizer Results

Using the Response Optimizer, an optimum parameter combination was determined that would both enhance ride comfort and maintain the tire-road contact force by minimizing the RMS body acceleration and objective function J within desired limits.

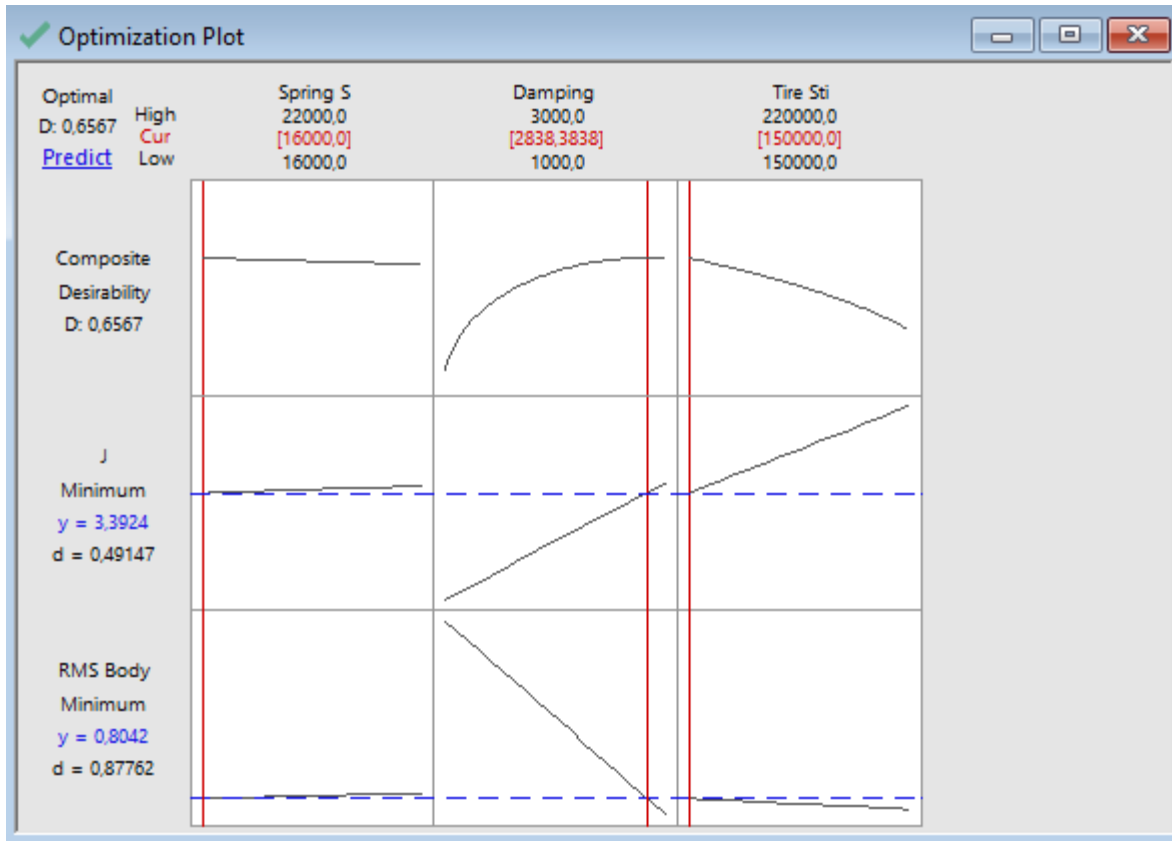


Figure 4.18 Response Optimizer Results

Figure 4.17 shows that the optimum suspension system parameters for ride comfort and handling are a coil spring stiffness of 16,000 N/m, a damper damping coefficient of 2,838.38 Ns/m, and a tire stiffness of 150,000 N/m.

The optimization plot presented above demonstrates the successful identification of a parameter combination that balances ride comfort and tire-road interaction performance. The primary objective of the optimization process was to minimize both the RMS value of body acceleration, which represents ride comfort, and the objective function J, defined as the ratio of the peak-to-peak value to the RMS of the tire-road contact force. In this context, the value of J serves as a key metric reflecting the dynamic consistency and stability of the contact force.

An analysis of the response plots clearly indicates that the damping coefficient is the most influential parameter affecting both the RMS and J outputs. Increasing the damping value significantly reduces body acceleration and contributes to a more stable contact force. This aligns with theoretical expectations, and the solution converges around a damping value of approximately

2838 Ns/m. This confirms the critical role of damping in dissipating energy efficiently and minimizing oscillatory motion in the system.

In contrast, spring stiffness and tire stiffness exhibit lower sensitivity, particularly in relation to RMS body acceleration, as evidenced by the nearly flat response curves. However, slight changes in tire stiffness still have a limited effect on the objective function J , suggesting that while these parameters are not the primary drivers, they may still serve to fine-tune the system response.

The composite desirability score of 0.6567 indicates a satisfactory balance between the two conflicting objectives. The obtained RMS body acceleration value of 0.8042 m/s² is close to the lower bound, while the objective function value of $J=3.3924$ demonstrates a notable reduction in the relative variability of the tire-road contact force.

In conclusion, the multi-objective optimization approach has led to a suspension configuration that effectively improves ride comfort while ensuring stable force transmission at the tire-road interface. The results clearly highlight the dominant influence of the damping coefficient on both comfort and dynamic force behavior, further validating the critical role of damping in suspension system design.

5. CONCLUSION

This thesis comprehensively investigates the dynamic behavior of a quarter-car suspension system both theoretically and experimentally. The mathematical model, developed based on Newton's second law of motion, was constructed in the Simulink environment using differential equations; the model was expressed in both state-space and transfer function forms. Additionally, the physical counterparts of the system were modeled, successfully achieving both abstract and physical representations.

The road input was simulated using a sinusoidal signal configured according to frequency and amplitude values specified in the literature, effectively replicating road irregularities. To numerically assess ride comfort, the RMS value of the body acceleration response of the sprung mass was calculated. Furthermore, the tire-road contact force was analyzed in terms of both peak-to-peak and RMS values; the variation of this force over time and its relationship with system parameters were examined in detail. The RMS and tire-road force data obtained from the model were validated through comparison with different solution approaches.

In the final phase of the thesis, Design of Experiments (DOE) methodology was applied to improve system performance, with analyses conducted using Minitab software. Suspension parameters (spring stiffness, damping coefficient, and tire stiffness) were varied at different levels, resulting in a total of eight scenarios modeled. The collected data were analyzed using a Pareto chart to identify the most influential parameters. Subsequently, the Response Optimizer tool was employed to examine the mean effect plots and successfully determine the optimal combination of parameters. This combination aimed to minimize the RMS value to enhance ride comfort while keeping the tire-road contact force within desired limits.

In conclusion, this thesis presents a holistic approach to the quarter-car suspension system by integrating modeling, analysis, experimental planning, and optimization, thereby providing a comprehensive solution process.

6. REFERENCES

- [1] Nekoui, Mohammed Ali; Hadavi, Parisa, «Optimal control of an active car suspension based on model from intelligent system identification,» %1 içinde *14th International Power Electronics and Motion Control Conference (EPE-PEMC)*, Ohrid, 2010.
- [2] D. Hanafi, «PID controller design for semi-active car suspension based on model from intelligent system identification,» %1 içinde *Second International Conference on Computer Engineering and Applications*, 2010.
- [3] Z. Wang, C. Liu, X. Zheng, L. Zhao ve Y. Qiu, «Advancements in Semi-Active Automotive Suspension Systems with Magnetorheological Dampers: A Review,» cilt 14, p. Art. no. 7866, 2024.
- [4] K. Jain ve R. Asthana, *Automobile Engineering*, New Delhi: Tata McGraw-Hill Publishing Company Limited, 2002.
- [5] M. Benaziz, S. Nacivet, J. Deak ve F. Thouverez, «Double Tube Shock Absorber Model for Noise and Vibration Analysis,» *SAE International Journal of Passenger Cars - Mechanical Systems*, cilt 6, no. 2, p. 1177–1185, July 2013.
- [6] R. N. Jazar, *Vehicle Dynamics: Theory and Application*, New York, NY, USA: Springer, 2008.
- [7] J. Fitch, *Motor Truck Engineering Handbook*, Society of Automotive Engineers, 1994.
- [8] A. Awasthi ve R. K. Ambikesh, «A Review Paper on Design and Analysis of Control ARM,» *i-manager's Journal on Mechanical Engineering*, cilt 11, no. 3, 2021.

- [9] Okuturlar, Himmet, «Numerical and Experimental Dynamic Analysis of A Vehicle Suspension System,» Necmettin Erbakan Üniversitesi, Fen Bilimleri Enstitüsü, Konya, 2018.
- [10] A. Çakan, «Karayolu Taşıtları Süspansiyon Sisteminde Aktif Titreşim Kontrolü,» Selçuk Üniversitesi, Fen Bilimleri Enstitüsü, Konya, 2013.
- [11] I. Mihai ve F. Andronic, «Behavior of a Semi-Active Suspension System Versus a Passive Suspension System on an Uneven Road Surface,» *Mechanika*, cilt 20, 2024.
- [12] H. Yong, J. Seo, J. Kim, M. Kim ve J. Choi, «Suspension Control Strategies Using Switched Soft Actor-Critic Models on Real Roads,» *IEEE Transactions on Industrial Electronics*, cilt 70, p. 824–832.
- [13] M. F. Aladdin ve J. Singh, «Modelling and Simulation of Semi-Active Suspension System for Passenger Vehicle,» *Journal of Engineering Science and Technology*, July 2016.
- [14] J. Sun ve Y. Sun, «Comparative study on control strategy of active suspension system,» %1 içinde *Third International Conference on Measuring Technology and Mechatronics Automation*, 2011.
- [15] T. D. Gillespie, Fundamentals of Vehicle Dynamics, Warrendale, PA: SAE International, 2021.
- [16] A. Agharkakli, G. S. Sabet ve A. Barouz, «Simulation and Analysis of Passive and Active Suspension System Using Quarter Car Model for Different Road Profile,» *International Journal of Engineering Trends and Technology*, cilt 3, no. 5, 2012.
- [17] J. Calvo, V. Díaz ve J. San Román, «Establishing inspection criteria to verify the dynamic behaviour of the vehicle suspension system by a platform vibrating test bench,» *Int. J. Vehicle Design*, cilt 38, 2005.

- [18] S. Lajqi ve S. Pehan, «Designs and Optimizations of Active and Semi-Active Non-linear Suspension Systems for a Terrain Vehicle,» *Strojniški vestnik – Journal of Mechanical Engineering*, cilt 58, no. 12, 2012.
- [19] P. Senthilkumar ve K. Sivakumar, «Fuzzy control of active suspension system,» *Journal of Vibroengineering*, 2016.
- [20] M. Hamed, «Characterisation of the Dynamics of an Automotive Suspension System for On-line Condition Monitoring,» Huddersfield, 2016.
- [21] S. Laqi, J. Gugler, N. Lajqi, A. Shala ve R. Likaj, «ossible Experimental Method to Determine the Suspension Parameters in a Simplified Model of a Passenger Car,» *International Journal of Automotive Technology*, cilt 13, no. 4, 2012.
- [22] S. A. Patil, «Experimental analysis of 2DOF quarter car passive and hydraulic active suspension systems for ride comfort,» *Systems Science and Control Engineering: An Open Access Journal*, cilt 2, p. 621–631, 2014.
- [23] N. S. Nise, *Control Systems Engineering*, 6. изд., Hoboken, NJ, USA: John Wiley & Sons, Inc., 2011.
- [24] S. S. Rao, *Engineering Optimization: Theory and Practice*, 4th изд., Hoboken, NJ, USA: John Wiley & Sons, 2009.
- [25] G. Llewelyn, A. Rees, C. Griffiths ve M. Jacobi, «A Design of Experiment Approach for Surface Roughness Comparisons of Foam Injection-Moulding Methods,» *Materials*, cilt 13, no. 10, 2020.
- [26] M. R. Abd-Elwahab, M. M. Makrahy, N. M. Ghazaly ve A. O. Moaaz, «Optimization and Analysis of the Quarter Car Passive Suspension Using Taguchi, Genetic Algorithm, and Simulated Annealing Approaches,» *International Journal of Transport and Device Innovation*, cilt 8, no. 3, 2024.

- [27] J. C. Dixon, *Tires, Suspension and Handling*, Second Edition dü., Warrendale, Pa.: Society of Automotive Engineers, Inc. (SAE), 1996.

7. APPENDICES

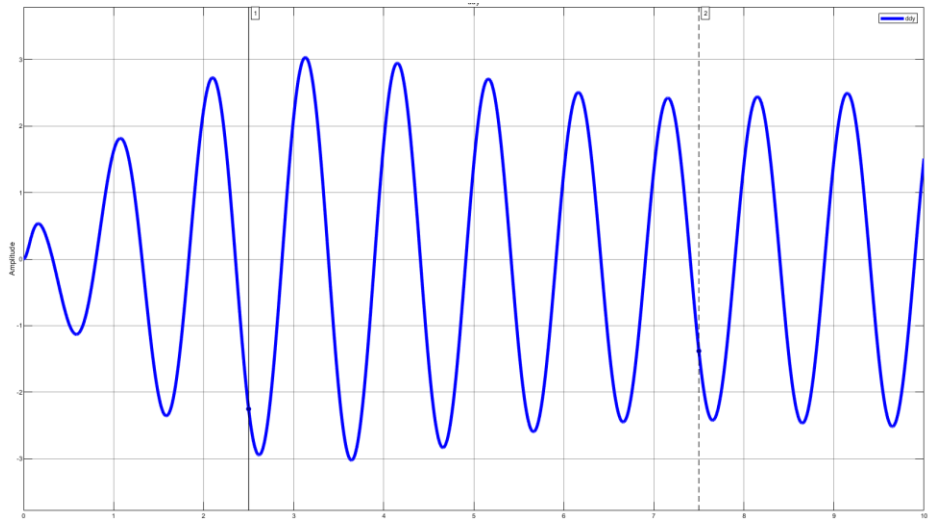


Figure 7.1 Graph for sprung mass acceleration with minimum variables

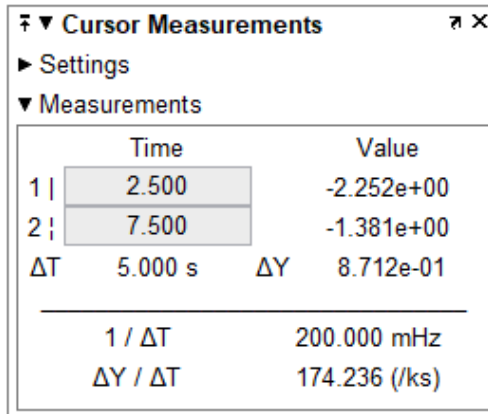


Figure 7.2 Cursor Measurements in Figure 7.1

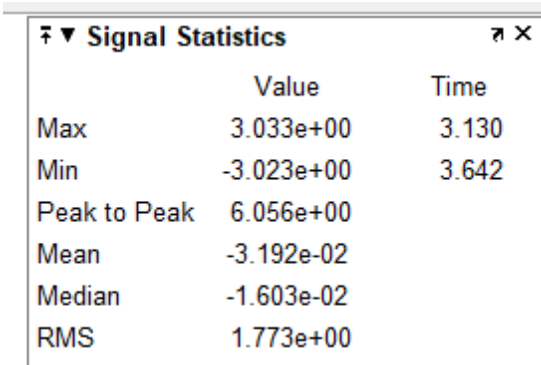


Figure 7.3 Signal Statistics in Figure 7.1

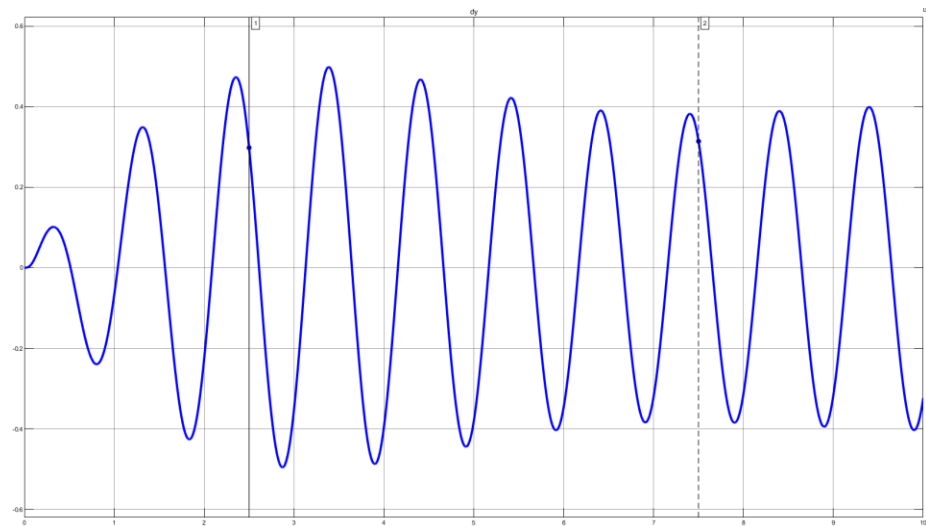


Figure 7.4 Graph for sprung mass velocity with minimum variables

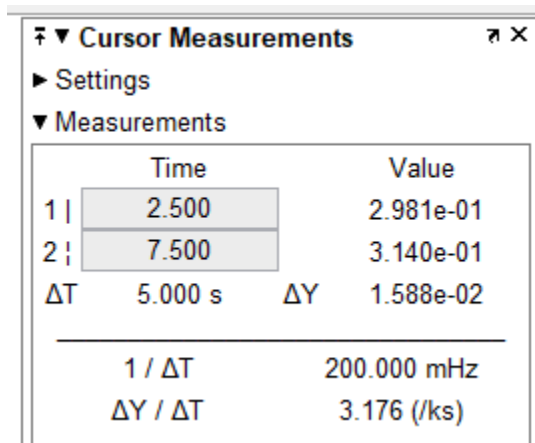


Figure 7.5 Cursor Measurements in Figure 7.4

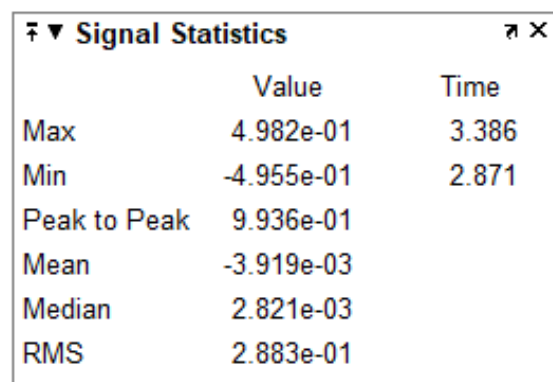


Figure 7.6 Signal Statistics in Figure 7.4

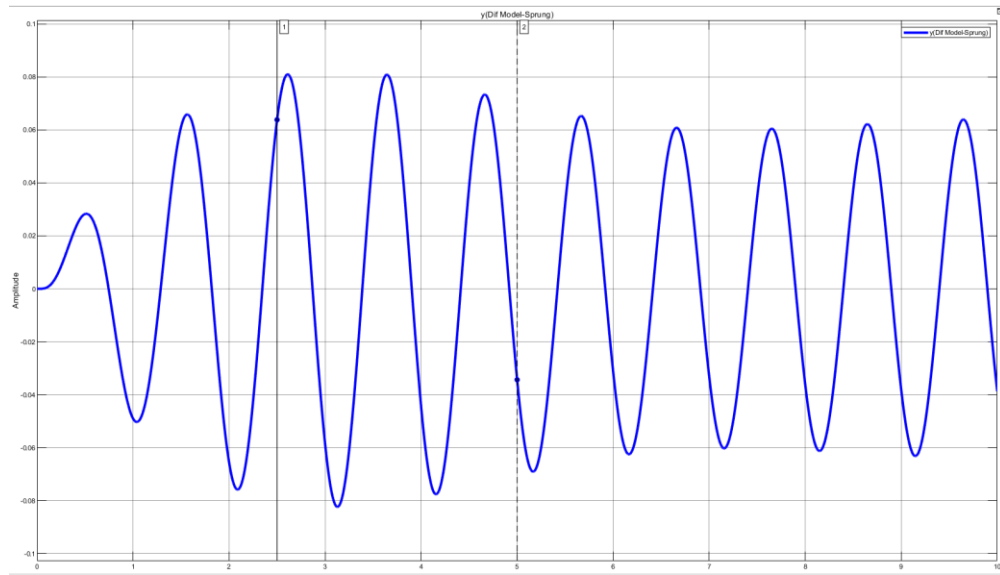


Figure 7.7 Graph for sprung mass displacement with minimum variables

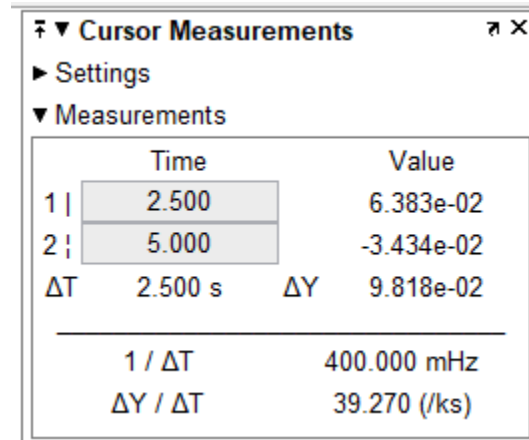


Figure 7.8 Cursor Measurements in Figure 7.7

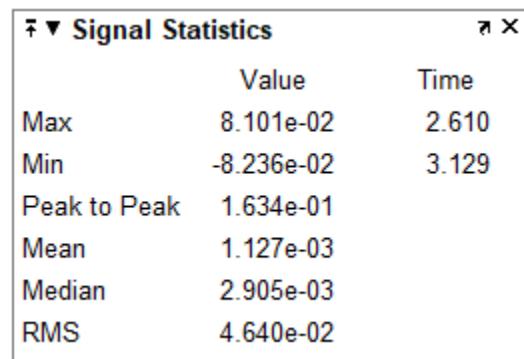


Figure 7.9 Signal Statistics in Figure 7.7

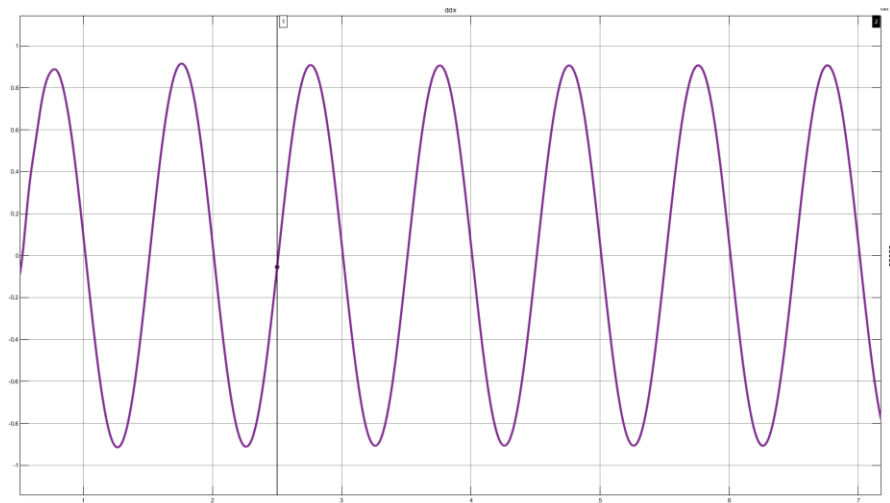


Figure 7.10 Graph for unsprung mass acceleration with minimum variables

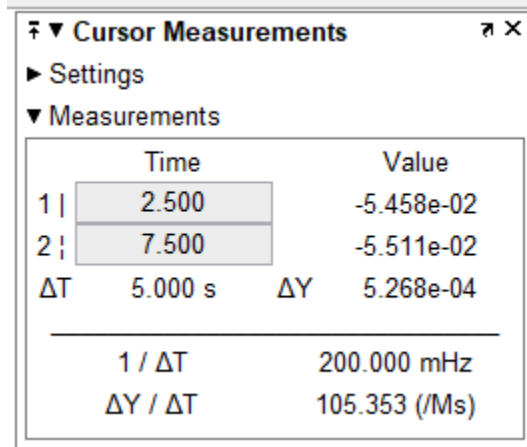


Figure 7.11 Cursor Measurements in Figure 7.10

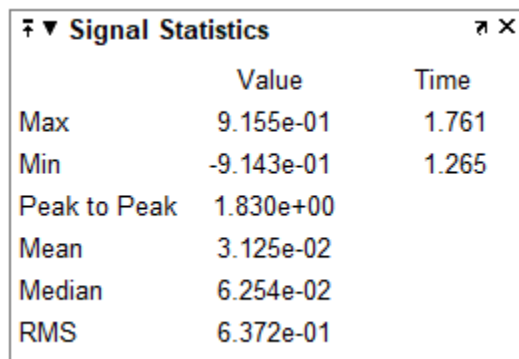


Figure 7.12 Signal Statistics in Figure 7.10

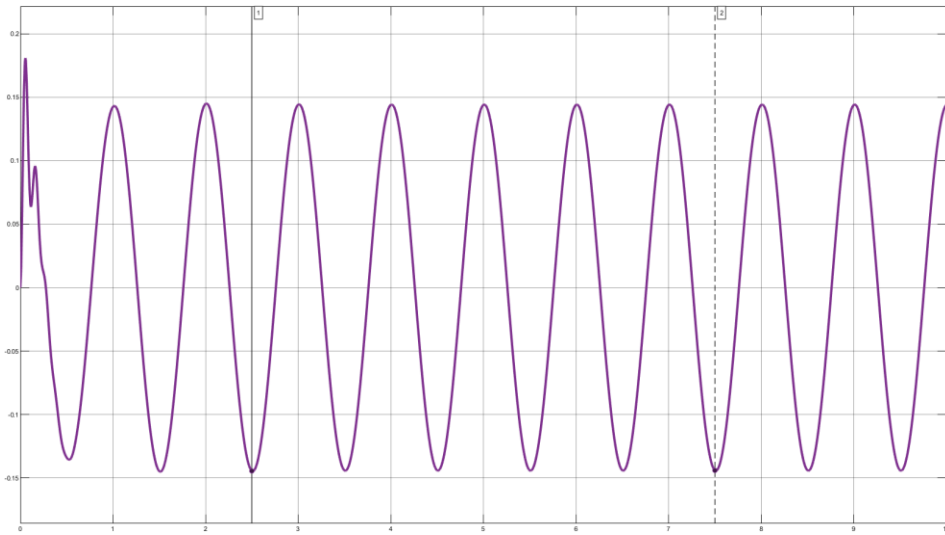


Figure 7.13 Graph for unsprung mass velocity with minimum variables

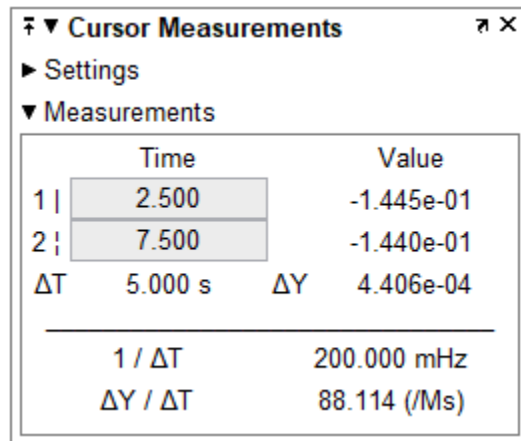


Figure 7.14 Cursor Measurements in Figure 7.13

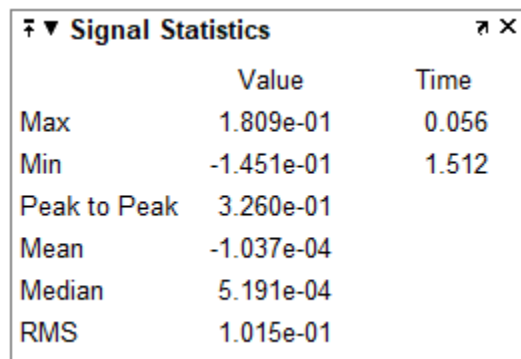


Figure 7.15 Signal Statistics in Figure 7.13

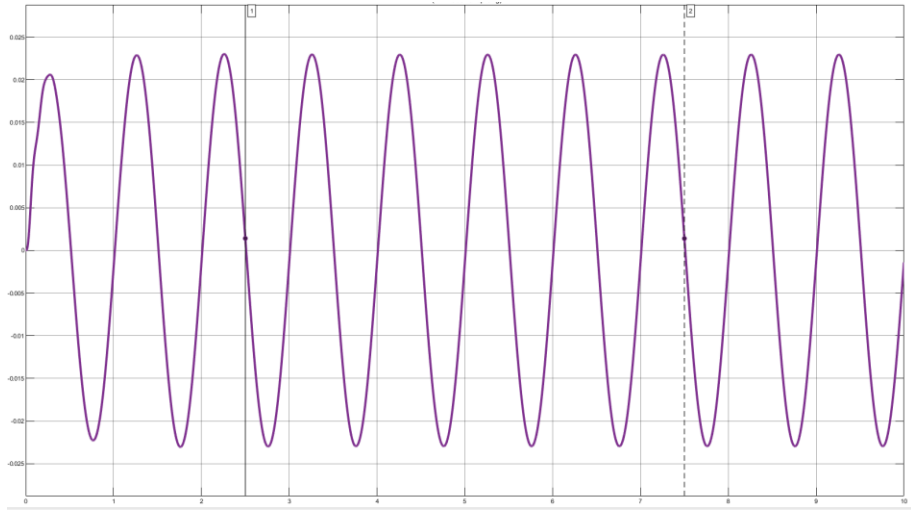


Figure 7.16 Graph for unsprung mass displacement with minimum variables

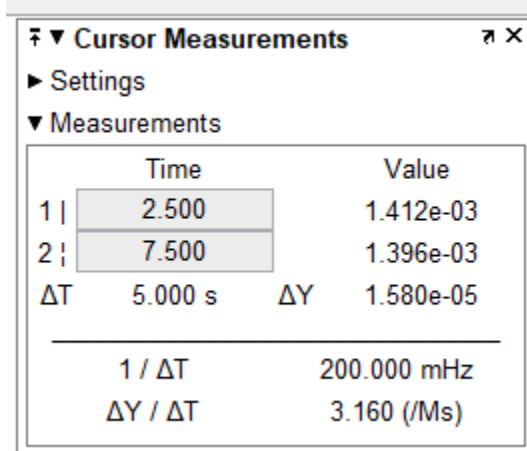


Figure 7.17 Cursor Measurements in Figure 7.16

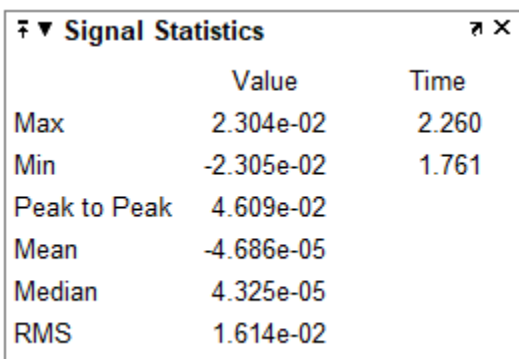


Figure 7.18 Signal Statistics in Figure 7.16

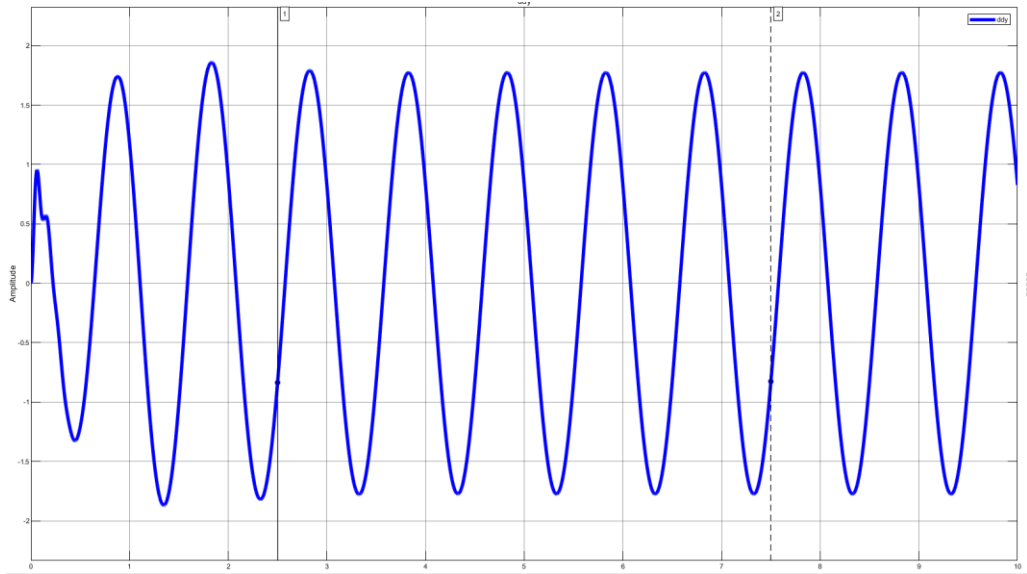


Figure 7.19 Graph for sprung mass acceleration with maximum variables

	Value	Time
Max	1.860e+00	1.831
Min	-1.869e+00	1.346
Peak to Peak	3.729e+00	
Mean	2.524e-02	
Median	5.466e-02	
RMS	1.243e+00	

Figure 7.20 Cursor Measurements in Figure 7.19

Cursor Measurements	
► Settings	
▼ Measurements	
1	Time Value
2	2.500 -8.361e-01
2	7.500 -8.265e-01
ΔT	5.000 s ΔY 9.587e-03
<hr/>	
1 / ΔT 200.000 mHz	
ΔY / ΔT 1.917 (/ks)	

Figure 7.21 Signal Statistics in Figure 7.19

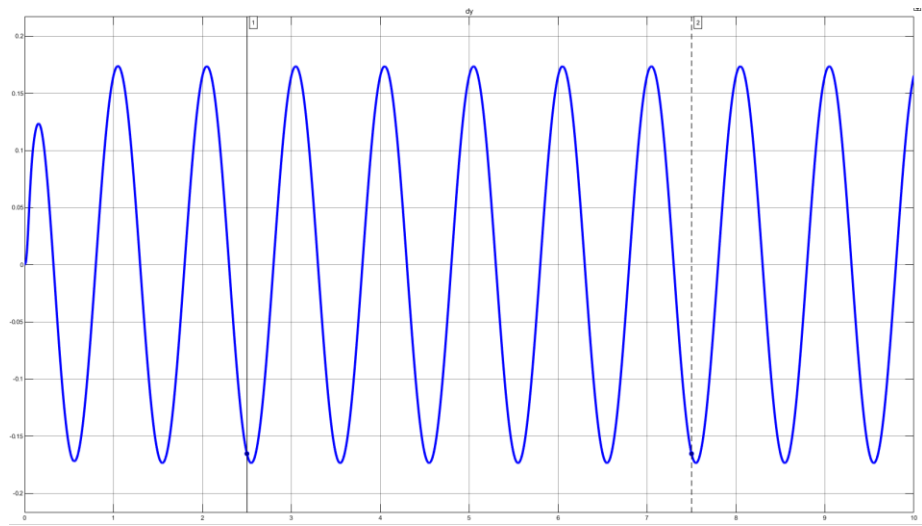


Figure 7.22 Graph for sprung mass velocity with maximum variables

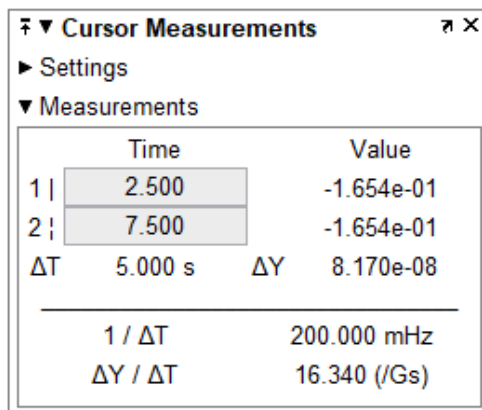


Figure 7.23 Cursor Measurements in Figure 7.22

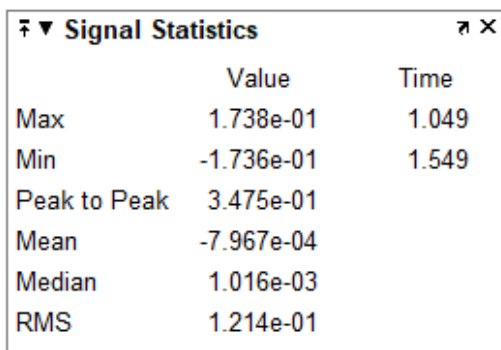


Figure 7.24 Signal Statistics in Figure 7.22

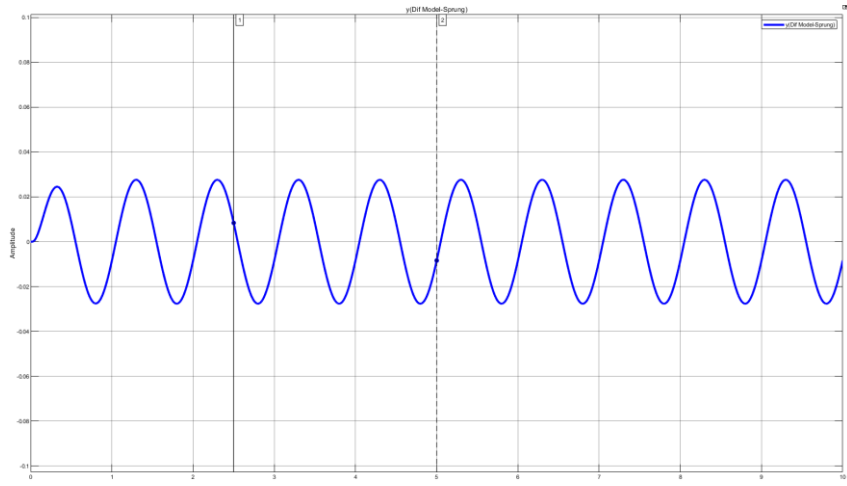


Figure 7.25 Graph for sprung mass displacement with maximum variables

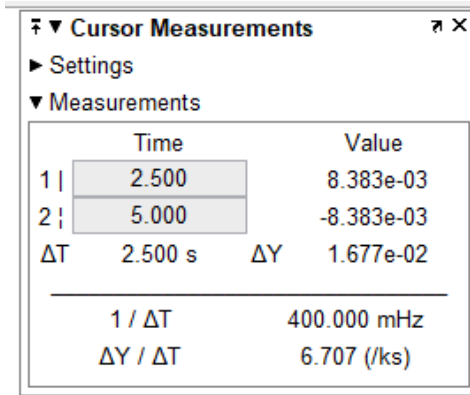


Figure 7.26 Cursor Measurements in Figure 7.25

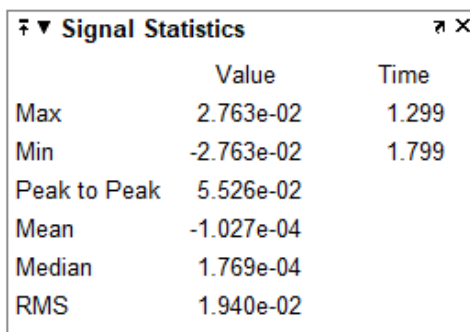


Figure 7.27 Signal Statistics in Figure 7.25

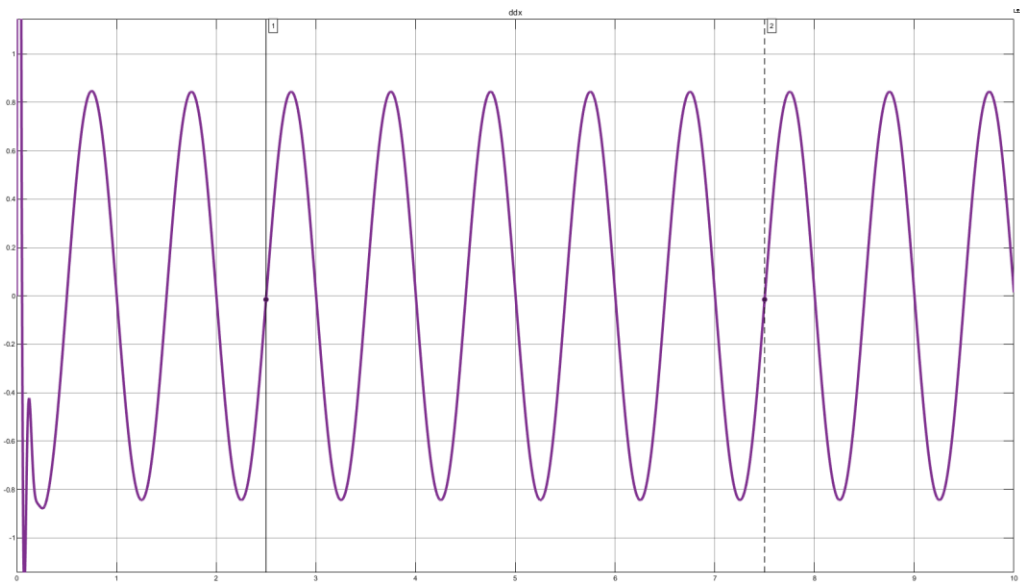


Figure 7.28 Graph for unsprung mass acceleration with maximum variables

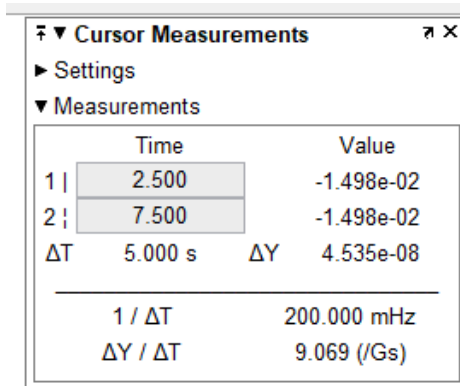


Figure 7.29 Cursor Measurements in Figure 7.28

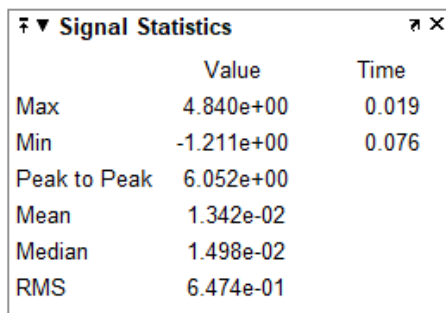


Figure 7.30 Signal Statistics in Figure 7.28

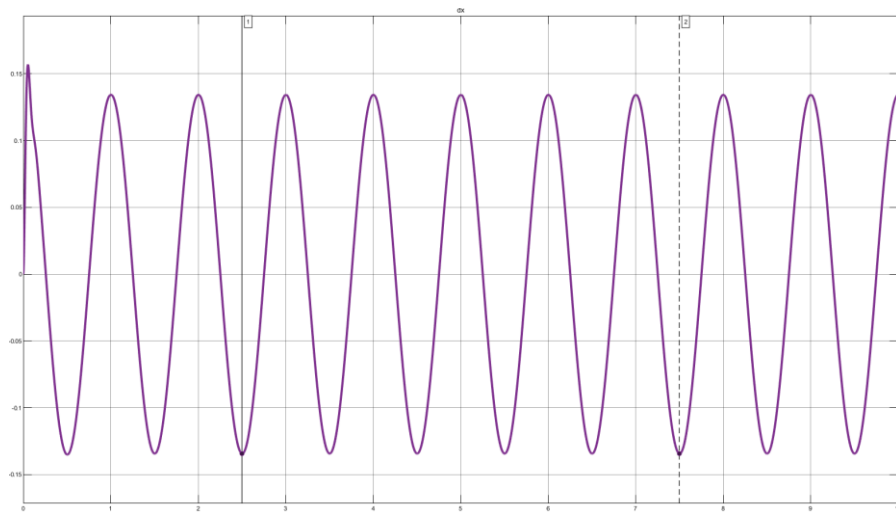


Figure 7.31 Graph for unsprung mass velocity with maximum variables

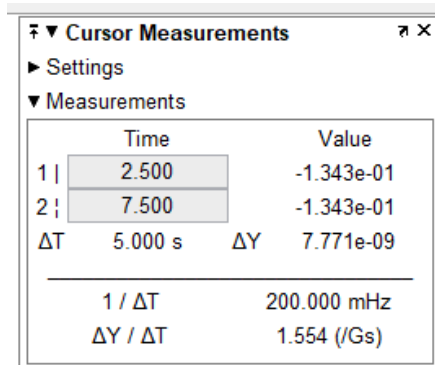


Figure 7.32 Cursor Measurements in Figure 7.31

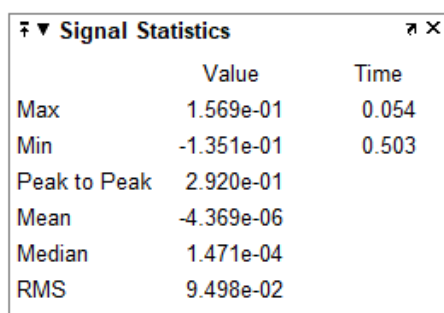


Figure 7.33 Signal Statistics in Figure 7.31

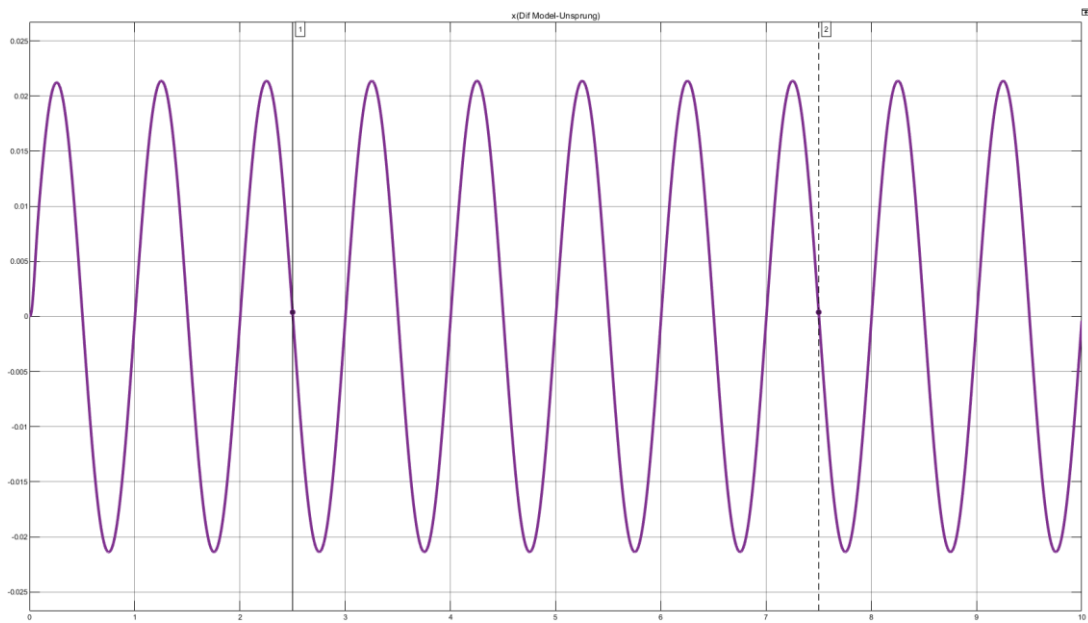


Figure 7.34 Graph for unsprung mass displacement with maximum variables

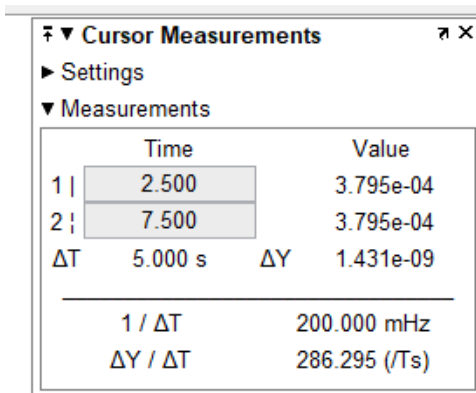


Figure 7.35 Cursor Measurements in Figure 7.34

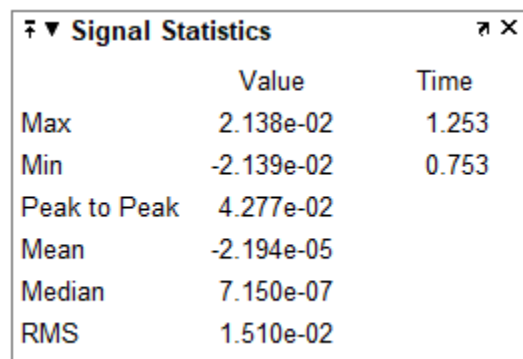


Figure 7.36 Signal Statistics in Figure 7.34

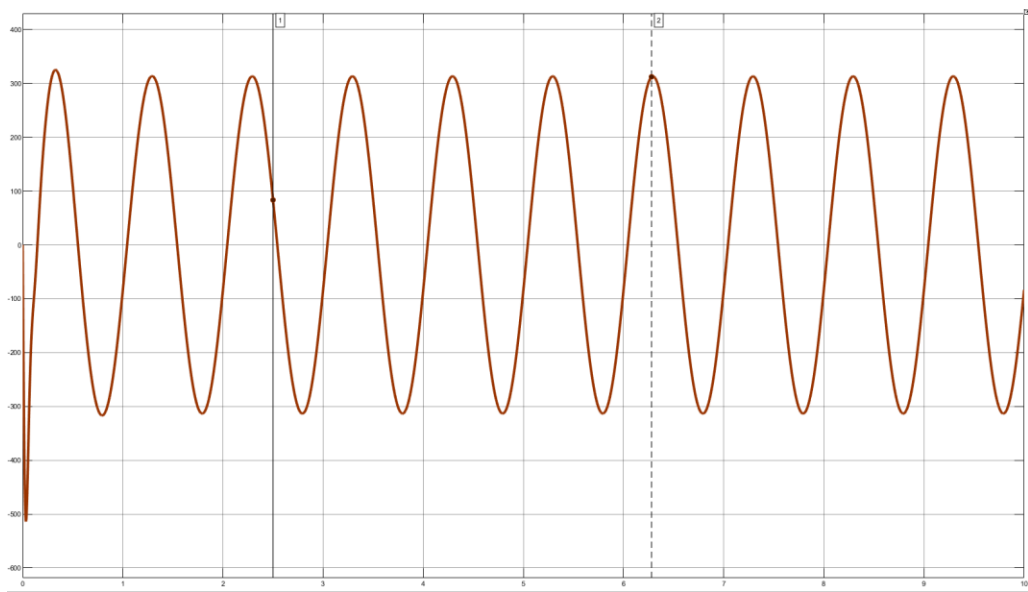


Figure 7.37 Graph for Tire Road Contact Force with maximum values

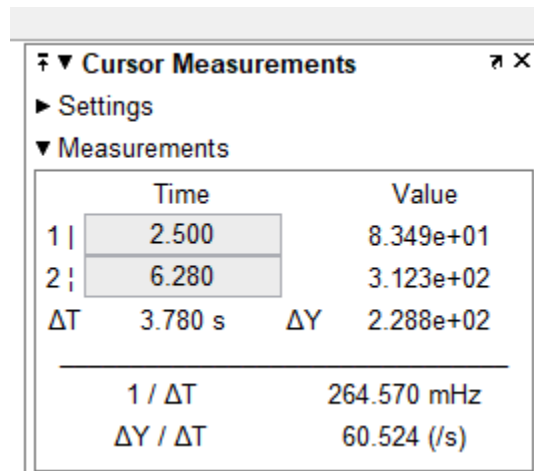


Figure 7.38 Cursor Measurements in Figure 7.37

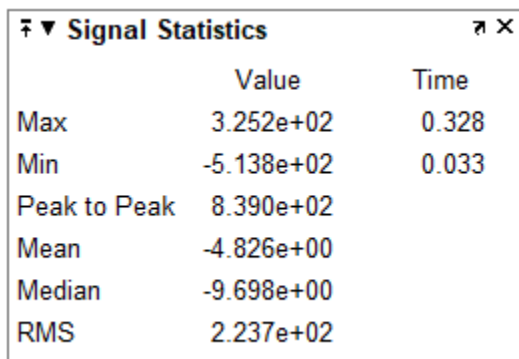


Figure 7.39 Signal Statistics in Figure 7.37

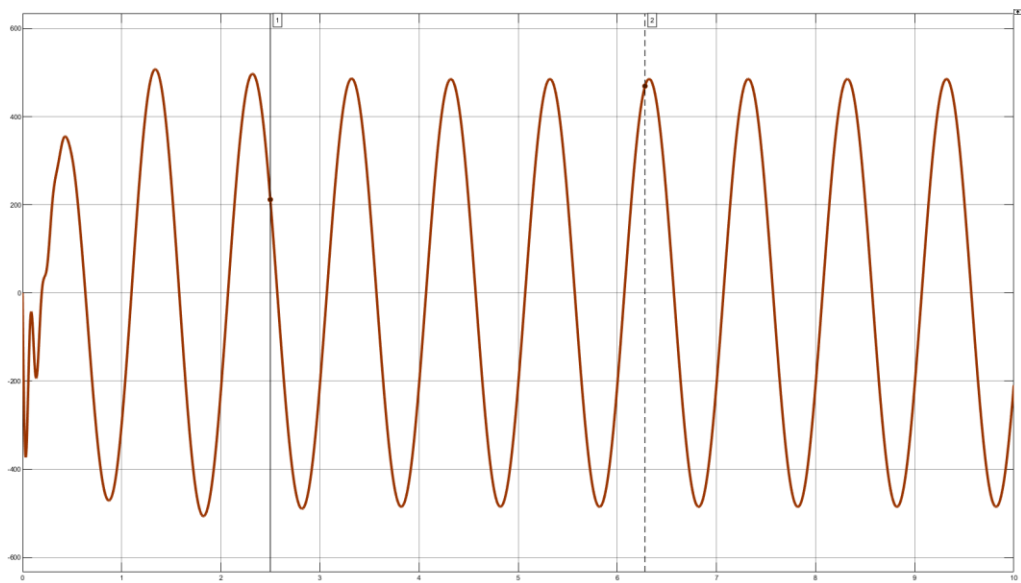


Figure 7.40 Graph for Tire Road Contact Force with minimum values

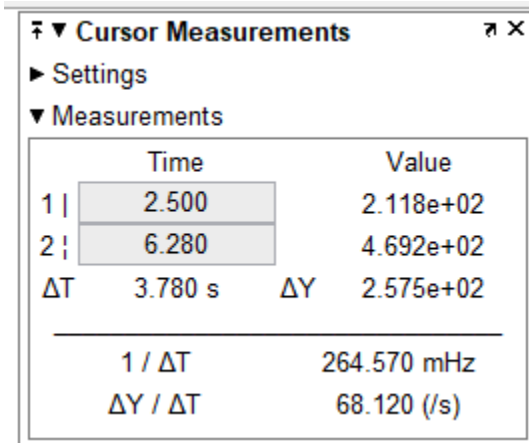


Figure 7.41 Cursor Measurements in Figure 7.40

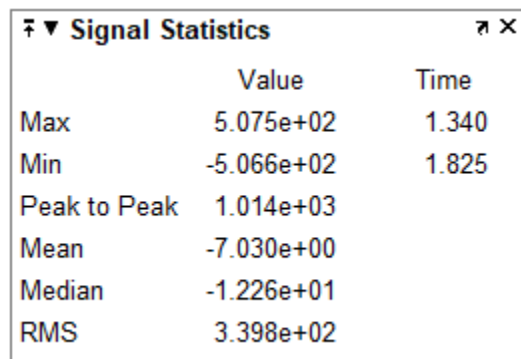


Figure 7.42 Signal Statistics in Figure 7.40